Economic Geology
Monograph 9, 1997, pp. 287–305

Epithermal Mercury-Antimony and Gold-Bearing Vein Lodes of Southwestern Alaska

JOHN E. GRAY, CAROL A. GENT, LAWRENCE W. SNEE,
U.S. Geological Survey, Federal Center, Denver, Colorado 80225

AND FREDERIC H. WILSON
U.S. Geological Survey, 4200 University Drive, Anchorage, Alaska 99508

Abstract

Epithermal mineral deposits and occurrences of southwestern Alaska consist of Hg-Sb and gold- and sulfide-bearing vein lodes. Numerous Hg-Sb lodes are located throughout a region measuring several tens of thousands of square kilometers in and surrounding the Kuskokwim River basin in southwestern Alaska. The Hg-Sb lodes are hosted in sedimentary rocks of the Cretaceous Kuskokwim Group, the Triassic to Cretaceous Gemuk Group, and the Paleozoic Holitna Group, as well as in Late Cretaceous and early Tertiary mafic to felsic intrusive rocks. Mineralized Hg-Sb vein and vein breccia lodes are found in the sedimentary or igneous rocks or at their contacts. The mineralogy of the Hg-Sb lodes is dominated by cinnabar and stibnite, with subordinate realgar, orpiment, native mercury, pyrite, gold, and hematite, as well as solid and liquid hydrocarbons; quartz, carbonate, limonite, dickite, and sericite are alteration gangue minerals. The largest mercury mine in Alaska, Red Devil, produced about 36,000 flasks of mercury, but the Hg-Sb lodes of southwestern Alaska generally consist of small, discontinuous veins that rarely exceed a few meters in width and a few tens of meters in strike length. The Hg-Sb lodes generally contain about 1 to 5 percent Hg and less that 1 percent Sb and As but are generally poor in base metals and precious metals. Anomalous concentrations of gold in some lodes, however, suggest that gold deposits may be present in higher temperature environments below some of the Hg-Sb lodes.

The formation of the Hg-Sb lodes is closely correlated with igneous activity of a Late Cretaceous and early Tertiary magmatic arc in southwestern Alaska. Geologic and geochemical characteristics of the Hg-Sb lodes suggest that ore fluids were generated in local sedimentary rocks as they were intruded by magmas. These intrusions provided the heat to initiate dehydration reactions and expel fluids from hydrous minerals and formational waters in the sedimentary rocks, causing thermal convection and hydrothermal fluid flow along fractures and faults. Isotopic data from sulfide and alteration minerals of the Hg-Sb lodes indicate multiple sources for the ore fluids; most fluids appear to have originated in local sedimentary rocks. Hydrothermal fluids with isotopically heavy oxygen but isotopically light hydrogen and sulfur compositions indicate derivation of these species from sedimentary rocks. Isotopically shifted, evolved meteoric water was a primary component in ore fluids from a few Hg-Sb lodes. Geochemical, isotopic, and fluid inclusion data also indicate that Hg, CO_2, CH_4, N_2, and local hydrocarbons were derived from breakdown of organic matter in sedimentary rocks when they were heated by intrusions. Radiometric $^{40}Ar/^{39}Ar$ ages of 70 $\pm$ 3 Ma from hydrothermal sericites in the Hg-Sb lodes indicate a temporal association of igneous activity and mineralization, which is consistent with the geologic characteristics.

Most epithermal gold-bearing vein lodes on the Alaska Peninsula and Aleutian Islands are located in Eocene to Pleistocene volcanic-arc rocks, commonly andesite and dacite. These vein and vein breccia lodes, such as the Alaska-Apollo and Shumagin deposits on Unga Island, tend to be aligned along regional, northeast-striking, steeply dipping faults and fractures. The Alaska-Apollo mine produced about 500,000 metric tons (t) of ore that yielded an estimated 3,500 kg (130,000 oz) of gold from veins that were as much as 12 m wide and extended for 1,500 m laterally and 420 m vertically. Ore minerals include gold, galena, sphalerite, chalcopyrite, pyrite, marcasite, arsenopyrite, and native copper; gangue minerals are quartz, sericite, calcite, and chlorite and locally, barite, clay, rhodonite, and adularia. Ores generally have Au-Ag-Te-Pb-Zn-Mn-Cu geochemical signatures, with wide As-Hg aureoles around some veins. Geologic and mineralogical characteristics of these lodes are similar to adularia-sericite volcanic-hosted epithermal deposits. The gold-bearing vein lodes may be related to arc porphyry systems, but more data are required to verify this association.

Introduction

EPITHERMAL lodes in Alaska consist of two broad types associated with specific regions: Hg-Sb vein lodes in the Kuskokwim River region of southwestern Alaska and gold- and sulfide-bearing vein lodes of the Alaska Peninsula and Aleutian Islands. Additional epithermal lodes are found in other parts of Alaska, such as the Hg-Sb-W vein lodes on the Seward Peninsula and in the Fairbanks area (Metz and Robinson, 1980). Some of these lodes have been described and mapped (Mertie, 1918a, 1918b; Hill, 1933; Metz, 1977), but lack of comprehensive, detailed studies of these additional lodes precludes further evaluation. Only the southwestern Alaska epithermal lodes are discussed in this study.

The Hg-Sb vein lodes of southwestern Alaska are scattered over several tens of thousands of square kilometers in the Kuskokwim River region (Fig. 1). Although this deposit type is one of the most poorly understood in Alaska, geologic, age, fluid inclusion, and isotopic data in this study indicate that Hg-Sb lodes are closely associated with Late Cretaceous and early Tertiary igneous rocks found in the region. Data also indicate that the Hg-Sb lodes of southwestern Alaska formed in a shallow epithermal environment (<250°C). These Hg-Sb lodes are possibly related to deeper level precious and

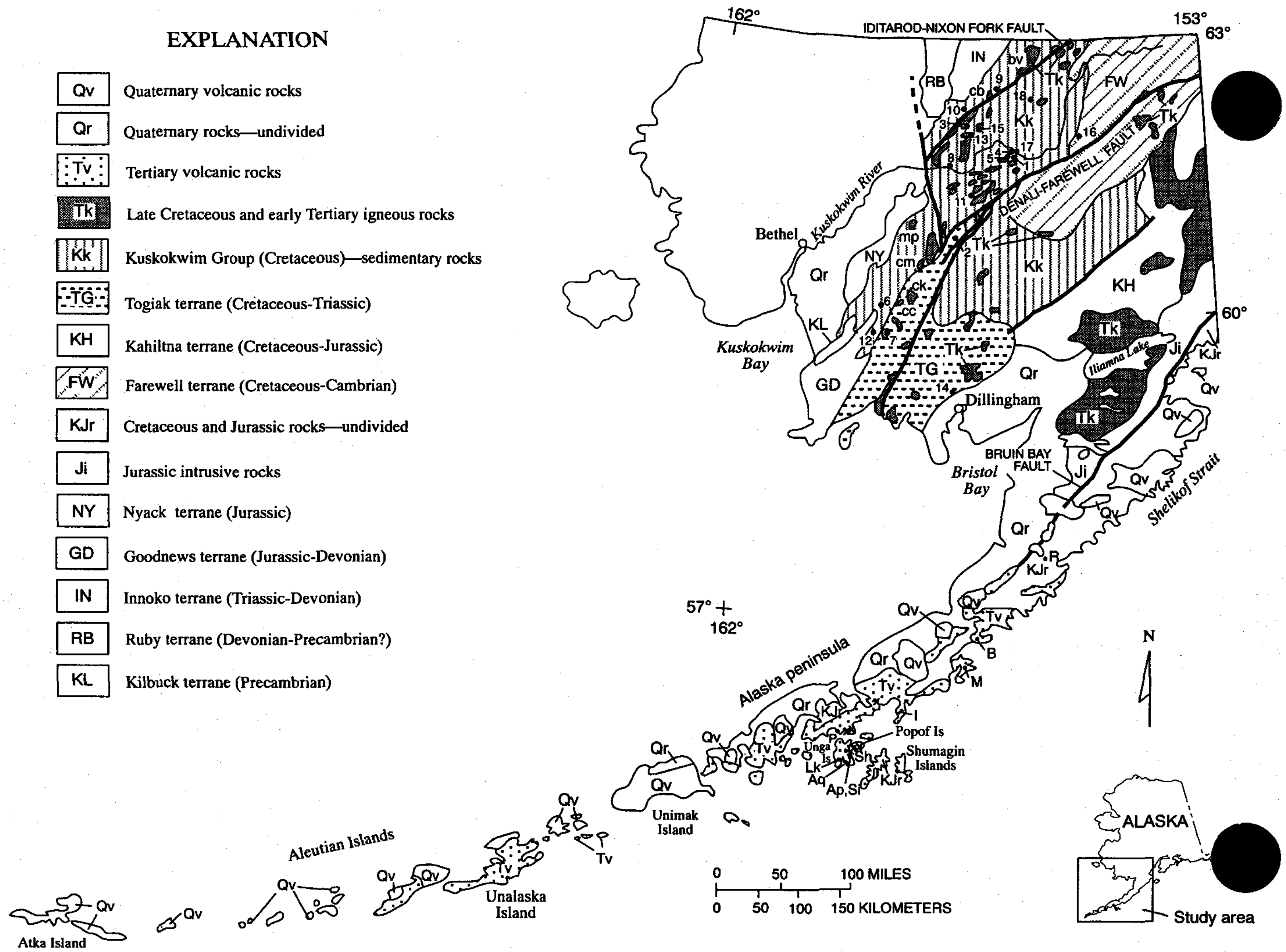

FIG 1. Map showing location of Hg-Sb mines and lodes and gold-bearing vein lodes in southwestern Alaska. Geology generalized from Cady et al. (1955), Hoare and Coonrad (1959), Jones et al. (1987), Miller et al. (1989), Box et al. (1993), Miller and Bundtzen (1994), and Wilson et al. (1996). See Table 1 for identification of numbered Hg-Sb mines and lodes. Abbreviations of plutons: bv = Beaver Mountains, cb = Chicken Mountain and Black Creek stock, cc = Canyon Creek, ck = Crooked Mountain, cm = Cripple Mountains, mp = Mount Plummer. Gold-bearing mines and vein lodes: Ap = Alaska-Apollo, Aq = Aquila, Lk = Lake prospect, Sh = Shumagin, Si = Sitka, × = other lodes. Porphyry deposits (shown for reference): B = Bee Creek, I = Ivanhoe, M = Mallard Duck, P = Pyramid, R = Rex.

base metal vein lodes found in the region that also show a close spatial association with Late Cretaceous and early Tertiary igneous rocks (Bundtzen and Miller, 1997).

Most of the Hg-Sb lodes are cinnabar rich (e.g., Red Devil) and are significant mercury resources, whereas other lodes are dominated by stibnite (e.g., Snow Gulch; Fig. 1). The first cinnabar lode in the region was discovered in 1838 by Russian traders on the Kuskokwim River at Kolmakof (no. 9, Fig. 1; Spurr, 1900). Since that time, numerous Hg-Sb lodes have been reported in the Kuskokwim River region (Mertie, 1936; Cady et al., 1955; Sainsbury and MacKevett, 1965). Early studies identified some of the southwestern Alaska Hg-Sb lodes and in some instances described the local geology (Spurr, 1900; Smith and Maddren, 1915; Mertie, 1936). Cady et al. (1955), MacKevett and Berg (1963), and Sainsbury and MacKevett (1965) were the first to synthesize the geology, mineralogy, and geochemical characteristics of these lodes.

Many of the Hg-Sb lodes have been mapped (e.g., Cady et al., 1955; MacKevett and Berg, 1963; Sainsbury and MacKevett, 1965; Sorg and Estlund, 1972). From the 1940s to the 1970s, the U.S. Bureau of Mines conducted drilling and trenching studies of many of the lodes, delineating size, grade, mineralogy, and ore distribution (e.g., Webber et al., 1947; Malone, 1962; Merrill and Maloney, 1974). Similar evaluations were conducted by the State of Alaska (Jasper, 1955) and by the U.S. Geological Survey (Sorg and Estlund, 1972). Prior to this study, however, there were no studies relating the timing and conditions of ore formation of these lodes to the regional geology. This paper presents geochemical, stable and radiogenic isotope, fluid inclusion, and age data for the Hg-Sb lodes in order to establish the geochemical and temporal conditions of formation and develop a genetic model for the lodes.

Several gold- and sulfide-bearing vein lodes are found the Alaska Peninsula and in the Aleutian Islands (Fig. 1; Collier, 1905; Atwood, 1911; Christie, 1974; Wilson et al., 1988; Randolph, 1991), but they have not been extensively studied. The best known of the gold lodes are Alaska-Apollo, Sitka, Shumagin, and Aquila on Unga Island in the Shumagin Islands (Fig. 1); several other smaller prospects and mineral occurrences are found on the southwestern Alaska Peninsula (Wilson et al., 1988; F.H. Wilson, unpub. data, 1994). These gold lodes were explored in the early 1900s and again in the 1980s and early 1990s (Mining Journal, 1987; Green et al., 1989). Several of the lodes have been mapped and drilled, and a few have had their reserves estimated, but little additional work has been done. Although there is still insufficient data to develop a comprehensive model of ore formation for these gold lodes, this report presents geologic, geochemical, and age data relevant to the framework geology of the Aleutian magmatic arc that hosts the lodes.

Regional Geology of Hg-Sb Vein Lodes

Southwestern Alaska Hg-Sb vein lodes are located in (1) Paleozoic, predominately carbonate rocks of the Holitna Group of the Farewell terrane, (2) Late Triassic to Early Cretaceous sedimentary and volcanic rocks of the Gemuk Group of the Togiak terrane, (3) postaccretionary Cretaceous clastic sedimentary rocks of the Kuskokwim Group, and (4) postaccretionary Late Cretaceous and early Tertiary mafic to felsic intrusions (Table 1). These Hg-Sb lodes show a close spatial association with the intrusions that cut the various rock types, and some are hosted in these igneous rocks.

The Holitna Group

White Mountain is the only Hg-Sb lode known in rocks of the Holitna Group of the Farewell terrane (no. 16, Fig. 1). The Holitna Group is a sequence of partly dolomitic, massive to thin bedded limestone, shale, calcareous sandstone, and minor intraformational conglomerate; fossils collected from rocks of the Holitna Group are Middle Cambrian to Middle Devonian (Cady et al., 1955; Sainsbury and MacKevett, 1965; Decker et al., 1994). Mineralized veins at White Mountain are in Ordovician black limestone, calcareous sandstone, argillaceous limestone, and shale (Sainsbury and MacKevett, 1965). Rocks of the Holitna Group represent shallow-water carbonate platform and deep-water shelf and slope facies of a continental margin sequence (Bundtzen and Gilbert, 1983; Blodgett and Clough, 1985). Rocks of the Farewell terrane are part of a passive continental margin sequence deposited on the flanks of the Precambrian North American crystalline continent during Paleozoic time that has moved little with respect to the American continent since the early Mesozoic (Bundtzen and Gilbert, 1983; Blodgett and Clough, 1985; Decker et al., 1994).

The Gemuk Group

The Cinnabar Creek and Red Top deposits are both located in rocks of the Gemuk Group of the Togiak terrane (Fig. 1; Jones et al., 1987). Rocks of this group are massive siltstones interbedded with lesser amounts of chert, andesitic flows and tuffs, and thin interbeds of graywacke, limestone, and breccia; these rocks represent deep-marine to shallow-water and subaerial facies (Cady et al., 1955; Miller et al., 1989). Fossils collected from rocks of the Gemuk Group are of Late Triassic and Cretaceous age (Cady et al., 1955). The Togiak terrane is interpreted to be part of a volcanic-arc complex accreted to North America during an arc-continent collision in the Late Cretaceous (Box, 1985; Decker et al., 1994).

The Kuskokwim Group

Most of the Hg-Sb lodes are hosted in sedimentary rocks of the Cretaceous Kuskokwim Group, which is a sequence of predominately flysch representing turbidite fan, foreslope, shallow-marine, and shelf facies deposited in an elongate, southwest-trending, fault-controlled Cretaceous basin (Decker and Hoare, 1982; Bundtzen and Gilbert, 1983; Miller and Bundtzen, 1994). Most of the sequence is composed of graywacke and shale, graywacke being approximately twice as abundant as shale (Cady et al., 1955). Conglomerate and interbeds of volcanic tuff and flow rocks are found locally (Cady et al., 1955; Miller and Bundtzen, 1994). Clast compositions of sandstone and conglomerate of the Kuskokwim Group indicate that the sources of sediment were local and that basin formation probably occurred near its present location (Bundtzen and Gilbert, 1983; Box and Elder, 1992; Miller and Bundtzen, 1994). The ages of fossils in these rocks range from Albian to Santonian (Cady et al., 1955; Box and Elder, 1992; Miller and Bundtzen, 1994), though an interbedded andesite tuff has a K/Ar age of 77 Ma (Campanian; Miller and Bundtzen, 1994). The Kuskokwim Group is postaccretionary, overlying rocks of adjacent tectono-stratigraphic terranes (Box et al., 1993; Miller and Bundtzen, 1994).

Late Cretaceous and early Tertiary igneous rocks

The Hg-Sb lodes are spatially associated with postaccretionary Late Cretaceous and early Tertiary igneous rocks that intrude or overlie rocks of the Holitna, Gemuk, and Kuskokwim Groups. These igneous rocks are volcanic-plutonic complexes; sheets, dikes, and sills of granite-porphyry; and intermediate to mafic dikes and sills (Cady et al., 1955; Bundtzen and Gilbert, 1983; Miller et al., 1989). Volcanic-plutonic complexes are volumetrically the most abundant, followed by granite-porphyry, and mafic to intermediate dikes. The Hg-Sb lodes are most commonly associated with granite-porphyry and intermediate to mafic dikes and sills. Rarely are the lodes associated with the volcanic-plutonic complexes, but this may be a result of erosion of the upper portions of these complexes.

Volcanic-plutonic complexes consist of volcanic rocks overlying or in fault contact with coeval plutons that intrude and partially assimilate the volcanic rocks (Bundtzen and Gilbert, 1983; Miller and Bundtzen, 1994). Minor stocks, dikes, and volcanic flow rocks are also thought to be related to the volcanic-plutonic rocks (Moll and Patton, 1982). Plutonic rocks of volcanic-plutonic association are most commonly monzonite, quartz monzonite, granodiorite, and granite; volcanic rocks consist of basalt, andesite, and rhyolite (Moll-Stalcup, 1994; Miller and Bundtzen, 1994). The K/Ar ages of the plutonic rocks range from 75 to 59 Ma, and associated volcanic rocks are dated at about 77 to 56 Ma (Shew and Wilson, 1981; Robinson and Decker, 1986; Miller and Bundtzen, 1994; Decker et al., 1995). Contact metamorphic aureoles surround

TABLE 1. Description of Hg-Sb Mines and Lodes in This Study

Mine or lode	Description	Mercury production (flasks)	References
1. Red Devil mine	Cinn-stib-qtz in altered diabase dikes and Kuskokwim Group graywacke and shale	36,000	2, 3, 4, 5, 11
2. Cinnabar Creek mine	Cinn-stib-Hg-qtz veins in altered graywacke and shale of the Gemuk Group and altered dikes	525	3, 5, 7, 11
3. Decourcy Mountain mine	Cinn-stib-qtz veins in altered diabase sills and Kuskokwim Group graywacke and shale	>1,200	2, 3, 5, 11
4. Barometer mine	Cinn-stib-real-orp-qtz veins in Kuskokwim Group graywacke and shale cut by altered dikes	16	2, 3, 5, 11
5. Fairview lode	Cinn-stib-qtz veins in granite-porphyry dike cutting Kuskokwim Group graywacke and shale	None	3, 5, 11
6. Fisher Dome lode	Stib-qtz veins in granite-porphyry dikes cutting Kuskokwim Group graywacke and shale	None	9, 11
7. Kagati Lake lode	Cinn-stib-real-orp-qtz veins in quartz monzonite and Gemuk Group graywacke and shale	None	5, 11
8. Kolmakof mine	Cinn-qtz-carb ± gold veins in altered dikes and Kuskokwim Group graywacke and shale	2	1, 3, 10, 11
9. McGimsey lode	Stib-qtz veins in Kuskokwim Group graywacke and shale cut by altered dikes	None	8, 11
10. Millers lode	Cinn-stib-qtz veins at contact of Kuskokwim Group shale and altered dike	None	8, 11
11. Mountain Top mine	Cinn-py-hycar-qtz veins in brecciated mafic dikes cutting Kuskokwim Group graywacke and shale	165	6, 11
12. Rainy Creek mine	Real-cinn-qtz veins in fractured Kuskokwim Group graywacke and shale and altered dikes	6	2, 5
13. Rhyolite lode	Cinn-qtz-carb veins in granite-porphyry dikes and Kuskokwim Group graywacke and shale	None	5, 11
14. Red Top mine	Cinn-qtz-carb veins in brecciated graywacke and siltstone of the Gemuk Group cut by altered dikes	>60	5, 11
15. Snow Gulch lode	Stib-py-qtz veins in granite-prophyry dike and Kuskokwim Group graywacke and shale	None[1]	3, 10, 11
16. White Mountain mine	Cinn-qtz-carb veins and cinn replacing Holitna Group limestone and shale cut by altered dikes	3,500	5, 7, 11
17. Willis mine	Cinn-stib-qtz veins at contact of altered dikes and Kuskokwim Group graywacke and shale	<10	1, 3, 5, 11
18. Granite Creek lode	Stib-qtz veins at contact of granite-porphyry dike with Kuskokwim Group graywacke and shale	None[2]	10, 11

References: 1. Smith and Maddren (1915); 2. Webber et al. (1947); 3. Cady et al. (1955); 4. MacKevett and Berg (1963); 5. Sainsbury and MacKevett (1965); 6. Sorg and Estlund (1972); 7. Nokleberg et al. (1987); 8. McGimsey et al. (1988); 9. Frost (1990); 10. Bundtzen and Miller (1997); and 11. this study

Abbreviations: carb = carbonate, cinn = cinnabar, Hg = liquid mercury, hycar = solid and liquid hydrocarbons, orp = orpimet, py = pyrite, qtz = quartz, real = realgar, stib = stibnite

[1] Placer mines in the area produced about 733 kg of gold

[2] About 100 kg of gold was produced from a placer mine downstream

the plutons where sedimentary and volcanic rocks are converted to hornfels.

Late Cretaceous and early Tertiary hypabyssal granite-porphyry and intermediate to mafic intrusions cut all rock types in the region. These intrusions are volumetrically minor, but they generally show a close spatial association with Hg-Sb lodes (Cady et al., 1955; Gray et al., 1992). Granite-porphyry intrusions are peraluminous in composition, locally containing garnet, and probably represent melted crust formed during emplacement of the volcanic-plutonic complexes (Miller and Bundtzen, 1994; Moll-Stalcup, 1994). Hypabyssal intermediate to mafic dikes and sills (typically composed of basalt, diabase, andesite, and gabbro) are generally altered to chalcedony, quartz, calcite, dolomite, sericite, and clay (Cady et al., 1955). The dikes are typically less than 1 m wide and are difficult to trace along strike for more than 10 m (Cady et al., 1955; Miller and Bundtzen, 1994). K/Ar ages for granite-porphyry range from 73 to 60 Ma (Robinson and Decker, 1986; Miller and Bundtzen, 1994; Decker et al., 1995); ages for mafic to intermediate dikes are poorly constrained because the rocks are commonly altered, but one dike has a K/Ar age of 71.2 ± 2.1 Ma (Miller and Bundtzen, 1994).

Tectonic setting

The Paleozoic Farewell and the Late Triassic and Cretaceous Togiak terrane boundaries generally parallel the southwestward-oriented structural and magmatic trend (Fig. 1). Rocks of the Kuskokwim Group overlap rocks of older terranes and were deposited in a Cretaceous basin that developed after accretion of the western Alaska terranes was completed in the mid-Cretaceous (Decker et al., 1994). Rocks of the Kuskokwim Group formed primarily by the deposition of local sedimentary detritus from turbidity currents into an elongate, fault-bounded basin. Rocks of the Kuskokwim Group are deformed into broad, open folds with local isoclinal folds and thrust faults (Decker et al., 1994; Miller and Bundtzen, 1994). Two major strike-slip faults, the Iditarod-Nixon Fork and the Denali-Farewell, dissect the region. Deformation and faulting probably began in the Late Cretaceous and continued into Tertiary time (Miller and Bundtzen, 1994). Structures observed by Miller and Bundtzen (1994) have been interpreted as part of a wrench-fault environment. Faults throughout southwestern Alaska may have controlled emplacement of the Late Cretaceous and early Tertiary plutonic and volcanic rocks (Miller and Bundtzen, 1994).

Comprehensive geochronologic, petrologic, isotopic, and major and trace element geochemical studies of the Late Cretaceous and early Tertiary igneous rocks in the region indicate that southwestern Alaska volcanic-plutonic complexes formed in a compressional subduction-arc environment (Wallace and Engebretson, 1984; Szumigala, 1993; Moll-Stalcup, 1994). This Late Cretaceous and early Tertiary magmatism is interpreted to be part of a broad belt of volcanic and intrusive rocks (extending from the Alaska Range to beyond the Kuskokwim Mountains) that formed in response to north-northeastward, gently dipping, rapid subduction of the Kula plate under southern Alaska (Engebretson et al., 1982; Wallace and Engebretson, 1984; Rea and Duncan, 1986; Wallace et al., 1989; Moll-Stalcup, 1994). Paleomagnetic data for the Late Cretaceous and early Tertiary rocks do not indicate significant northward translation of these rocks relative to North America (Globerman and Coe, 1982), which suggests that they formed near their present locations; paleomagnetic results also indicate 30° to 55° of counterclockwise rotation of these rocks since the Paleocene (Hillhouse et al., 1985; Thrupp and Coe, 1986).

Moll-Stalcup (1994) indicates that the Late Cretaceous and early Tertiary rocks (about 75–56 Ma) are subduction related, have a calc-alkaline to shoshonitic composition, and constitute an unusually wide magmatic arc. This arc initially consisted of the Alaska Range, the Talkeetna Mountains, and the Kuskokwim Mountains from 75 to 66 Ma but broadened to include the Yukon-Kanuti belt from 65 to 56 Ma (Moll-Stalcup, 1994). However, Bundtzen and Miller (1997) suggest that extension related to wrench-fault tectonics, rather than magmatic-arc tectonics, best explains structures and igneous rocks in southwestern Alaska.

Characteristics of the Hg-Sb vein lodes

The Hg-Sb lodes have a close spatial association with Late Cretaceous and early Tertiary mafic to felsic intrusions that cut the sedimentary rocks, where the lodes are found in the sedimentary and igneous rocks, or at their contacts (Cady et al., 1955; Herreid, 1960; Sainsbury and MacKevett, 1965). The lodes commonly consist of mineralized veins and vein breccias (Fig. 2A), but minor stockworks, replacements, and disseminations are also present. Cinnabar and stibnite are the dominant minerals; less abundant are realgar, orpiment, pyrite, native mercury, gold, and hematite (MacKevett and Berg, 1963; Sainsbury and MacKevett, 1965; Gray et al., 1990). Cinnabar and stibnite are commonly found in open-space fillings (Fig. 2B) in quartz-rich veins that also contain carbonate, limonite, dickite, and kaolinite gangue minerals; minor solid and liquid hydrocarbons and sericite are present locally. Mineral relationships indicate that the common paragenetic sequence is early carbonate and quartz, followed by pyrite, realgar, stibnite, cinnabar, and native mercury; dickite is generally a late-stage mineral. In some instances, stibnite formed later than cinnabar. A late, ore-stage variety of quartz intergrown with cinnabar is present in most lodes (Fig. 3). Macroscopic observations of samples collected from the Red Devil and Kolmakof mines indicate that gold was deposited with cinnabar. Sericite, when present, is typically coeval with cinnabar. Late-stage carbonate-bearing veins are found at many localitites. Limonite is supergene in origin.

The Hg-Sb lodes are generally found as small, discontinuous mineralized veins that are typically less than 2.5 cm wide but occasionally reach 1 m in width and several tens of meters in length, such as those observed at Red Devil (Sainsbury and MacKevett, 1965). Ore reserves have not been determined for a majority of the lodes. Although most of the Hg-Sb lodes are small, mercury grades can exceed 50 percent. Generally, however, ores contain about 1 to 5 percent Hg and less that 1 percent Sb and As (Webber et al., 1947; MacKevett and Berg, 1963; Sainsbury and MacKevett, 1965). Lodes mined were generally retorted on-site, and most produced only a few flasks of mercury (1 flask = 76 lbs or 34.5 kg). For example, about 16 flasks of mercury were produced from the Barometer mine, near Sleetmute (Cady et al., 1955). The exception is the Red Devil mine, the largest mercury mine in Alaska, from which about 36,000 flasks of mercury were recovered (Miller et al., 1989). In southwestern Alaska, the moderately sized Decourcy Mountain and Cinnabar Creek mines produced about 1,200 and 525 flasks, respectively. Approximately 41,000 flasks of mercury have been recovered from mines in southwestern Alaska since 1889 (Table 1), which is about 99 percent of the mercury produced in Alaska.

Some mineralized veins contain anomalous concentrations of gold and silver (Table 2; Hawley et al., 1969; Gray et al., 1990; Bundtzen et al., 1993; Bundtzen and Miller, 1997). Gold has been identified in detrital cinnabar nuggets collected downstream from Hg-Sb lodes (Cady et al., 1955) and in crushed heavy mineral concentrates of ore samples collected from a few localities (Gray et al., 1990). Ores from the Hg-Sb lodes are generally base metal poor (Gray et al., 1991). Anomalous concentrations of Hg, Sb, and As in mineralized vein and stream sediment samples and detrital cinnabar in heavy mineral concentrate samples are the most effective indicators when prospecting for these Hg-Sb vein lodes (Gray et al., 1991).

Regional geology and tectonic setting of the epithermal gold vein lodes

The Alaska Peninsula and Aleutian Islands are part of a number of subduction-related arcs that intermittently have been magmatically and seismically active since the Jurassic. Cenozoic magmatic rocks are the most economically important lithological units in the area, because they host epithermal gold-bearing vein lodes. Cenozoic rocks have been divided into calc-alkaline and tholeiitic rocks of Eocene to early Miocene age, which define the Meshik magmatic arc, and late Miocene and younger calc-alkaline to tholeiitic rocks of the Aleutian arc (Wilson, 1985; Wilson and Shew, 1992; Vallier et al., 1994).

On the Alaska Peninsula and Aleutian Islands, rocks of the Meshik arc include volcanic rocks and hypabyssal intrusions of basaltic to rhyolitic compositions yielding conventional K/Ar ages between 54 and 22 Ma and Eocene to early Miocene intercalated volcaniclastic rocks of the Stepovak Formation (Burk, 1965; Wilson, 1985; Vallier et al., 1994). The Meshik volcanics were originally described (Meshik Formation) as a sequence of reversely graded andesitic volcaniclastic rocks that include interbedded bentonitic clay, fine sand, volcanic ash, and coarse agglomerate; the upper part of the Meshik volcanics is composed of agglomerate and numerous flows (Knappen, 1929). Sedimentary rocks of the Meshik Vol-

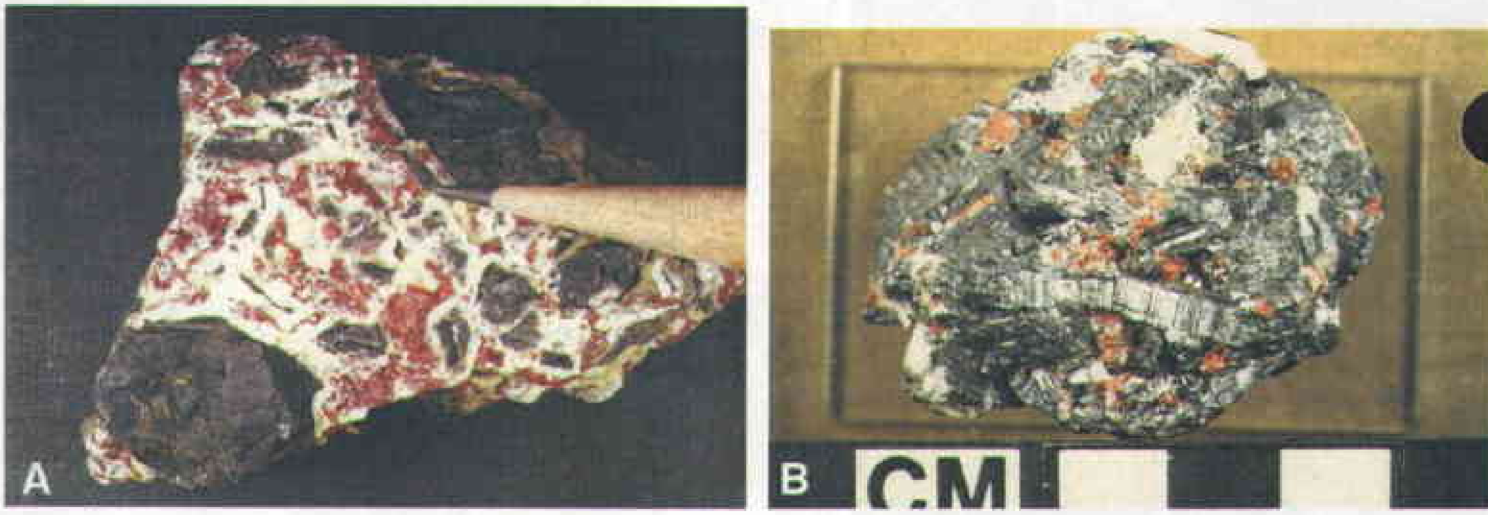

FIG. 2. Cinnabar-quartz veins (A) are the most common type of Hg-Sb lode in southwestern Alaska. Cinnabar and stibnite open-space fillings (B) are also typical in Hg-Sb lodes.

FIG. 3. Photomicrograph (1 cm wide) of intergrown vein cinnabar and hydrothermal quartz (arrow) from Red Devil, illustrating their coeval nature.

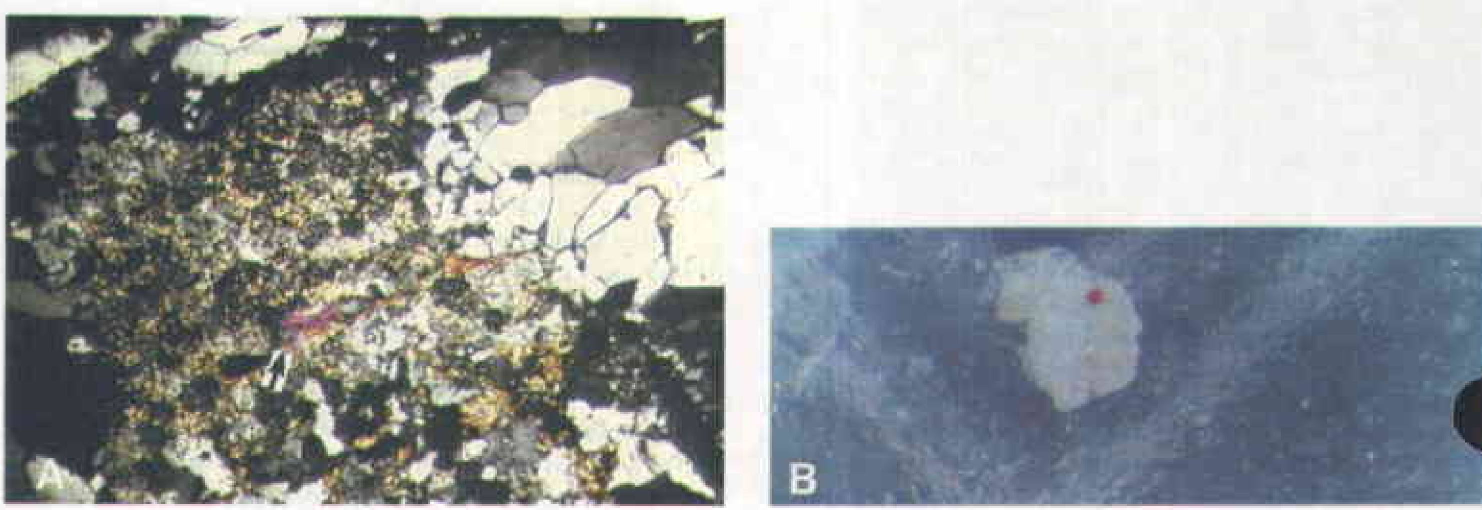

FIG. 4. Photomicrograph in cross polarized light showing minor hydrothermal sericite (A) adjacent to vein quartz in altered wall rock (width is 1 cm). Cinnabar intergrown with hydrothermal sericite from the Fairview prospect (B) indicates their coeval relationship. Sericite grain is about 100 μm in diameter.

TABLE 2. Trace Element Concentrations in Mineralized Rock Samples from Selected Mines

Sample[1]	Hg	Sb	As	Ag	Au	Cd	Cu	Mo	Pb	Zn
RD1	>10,000	2,200	73	<0.07	0.66	0.04	<0.03	0.17	<0.7	<0.02
RD1C	ND	>8,000	>3,000	0.26	4.4	0.22	12	0.27	9.2	<0.03
RD1D	ND	>8,000	390	0.45	1.1	0.15	8.8	0.29	11	<0.03
RD2	>10,000	7,700	130	<0.07	1.5	<0.02	<0.02	<0.06	<0.07	<0.02
RD3	>10,000	>9,300	44	<0.07	1.3	<0.02	<0.02	<0.06	<0.7	<0.02
RD4	>10,000	>9,300	230	<0.07	0.2	<0.02	<0.02	<0.06	<0.7	<0.02
CC1B	ND	13	94	<0.07	<0.002	0.09	2.7	0.15	1.2	<0.03
CC50	ND	>10,000	7,000	ND	0.40	ND	ND	ND	ND	ND
MT1C	ND	4	7.3	0.12	0.32	0.13	<0.03	0.31	1.5	<0.03
KM1	>10,000	12	<0.7	0.15	0.064	0.12	7.9	0.13	3.3	<0.02
KM2	>10,000	7	<0.7	0.10	0.005	0.08	1.6	0.28	1.0	<0.02
KM3	>10,000	130	17	13	87	0.35	53	0.31	11	<0.02
KM4	>10,000	200	54	38	150	0.32	66	1.4	18	3.4
BR1	>10,000	>9,300	>1,800	<0.07	0.41	<0.02	<0.02	<0.06	<0.7	<0.02
BR2	>10,000	>4,700	>1,800	<0.07	0.51	<0.02	7.3	<0.06	<0.7	<0.02
BR3	>10,000	>9,300	410	<0.07	1.1	<0.02	52	<0.06	<0.7	<0.02
BR4	>10,000	>9,300	780	<0.07	1.6	<0.02	13	<0.06	1.8	<0.02
FV1	>10,000	>9,300	480	<0.07	0.012	<0.02	<0.02	<0.06	<0.7	<0.02
FV2	>10,000	>9,300	170	<0.07	0.009	<0.02	<0.02	<0.06	<0.7	<0.02
FV3	>10,000	>9,300	52	<0.07	0.007	<0.02	<0.02	<0.06	<0.7	<0.02
FV4	>10,000	>9,300	60	<0.07	0.006	<0.02	<0.02	<0.06	<0.7	<0.02
RY1	>10,000	120	90	0.79	0.005	0.12	23	0.15	4.4	<0.02
RY2	>10,000	1,800	150	0.41	0.15	0.12	18	0.71	6.0	5.2
RY3	>10,000	480	200	0.31	0.76	0.09	24	0.59	5.6	31
RY4	>10,000	27	140	0.68	0.005	0.15	31	0.53	8.5	15
WL1	>10,000	2,500	11	0.16	0.004	0.13	6.2	0.08	2.3	<0.02
WL2	>10,000	210	32	0.19	0.008	0.08	1.3	0.18	0.95	<0.02
WL3	>10,000	>9,300	250	<0.07	1.8	<0.02	<0.02	<0.06	<0.7	<0.02
WL4	>10,000	>9,300	380	<0.07	0.28	<0.02	<0.02	<0.06	<0.7	<0.02
WM1A	ND	18	20	0.09	0.37	0.11	<0.03	0.28	1.5	<0.03

Analysis of Hg by cold vapor atomic absorption spectrophotometry; Sb, As, Ag, Cd, Cu, Mo, Pb, and Zn by inductively coupled plasma spectrometry; Au by atomic absorption spectrophotometry; concentrations are in ppm

[1] Abbreviations: BR = Barometer mine, CC = Cinnabar Creek, FV = Fairview lode, KM = Kolmakof mine, MT = Mountain Top mine, RD = Red Devil mine, RY = Rhyolite lode, WL = Willis mine, WM = White Mountain mine

ND = not determined

canics are shale, siltstone, and conglomerate whose clasts are predominantly volcanic fragments (Wilson, 1985). Volcanic rocks are typically dacitic to basaltic flows, agglomerate, and breccia (Wilson, 1980); however, minor rhyolite is present on Unga Island and the Alaska Peninsula. Basalt, andesite, and dacite intrusions cut genetically related flows of the Meshik volcanics (Wilson, 1985), as do uncommon granodiorite and quartz diorite plutons. Many hypabyssal intrusions and volcanic rocks show minor deuteric or hydrothermal alteration, typically containing epidote and chlorite.

Rocks of the Meshik arc are more than 1,500 m thick and are unconformably overlain by middle Miocene volcaniclastic rocks of the Bear Lake Formation and Unga Formation or by late Miocene volcaniclastic rocks that contain clasts of the Meshik arc rocks (Wilson, 1985). Overlying rocks of the Bear Lake Formation are plutonic, volcanic, and volcaniclastic rocks of the present-day Aleutian arc, including the Milky River Formation and plutons of the Devils, Agripina Bay, and other batholiths. K/Ar ages indicate that magmatic activity of the Aleutian arc began in the latest Miocene and has continued to the present (Wilson, 1981). Epithermal gold-bearing vein lodes on the Alaska Peninsula and Aleutian Islands are not known to be present in rocks of the Aleutian arc.

The dominant structures on the Alaska Peninsula and Aleutian Islands are northeast-striking, high-angle thrust faults that are generally subparallel to the trend of the Alaska Peninsula (Wilson et al., 1985). Most of the thrust faults place Mesozoic rocks against upper Miocene rocks (Wilson et al., 1996). The Bruin Bay fault is the most prominent thrust fault in the region (Fig. 1) and was probably active intermittently from the Jurassic to the middle Tertiary (Burk, 1965). Northeast-trending regional folds commonly parallel the thrust faults and are probably related to the thrust faults (Wilson et al., 1996). Oligocene rocks near the southern end of the Alaska Peninsula are tightly folded, but adjacent Miocene rocks are flat lying. Miocene rocks south of the Bruin Bay fault are gently folded (Wilson et al., 1996).

Local geology and characteristics of the gold vein lodes

Epithermal gold-bearing lodes on the Alaska Peninsula and Aleutian Islands are predominantly fault- and fracture-controlled vein and vein breccia lodes (Atwood, 1911; Wilson et al., 1988). Known lodes are present in Eocene to early Miocene, generally andesitic volcanic rocks and less commonly in small intrusions and volcaniclastic rocks (Wilson et al., 1988). The Alaska-Apollo deposit on Unga Island exemplifies this deposit type. Gold-bearing quartz veins of the Alaska-Apollo deposit strike N 20° E, dip steeply southward, and are hosted by Oligocene andesite (Atwood, 1911; Brown, 1947; Wilson et al., 1988). Veins are as much as 12 m wide and extend up to 1,500 m laterally and 420 m below the surface (Brown, 1947). The Alaska-Apollo mine produced about 3,500 kg (130,000 oz) of gold from an estimated 500,000 t of ore between 1891 and 1908 (Atwood, 1911; Wilson et al., 1988) and is the only mine on the island with significant production. Other smaller lodes in the region have also been explored; the Shumagin deposit, for example, has estimated reserves of about 270,000 t of ore grading 576 ppm Au and 2,332 ppm Ag (Mining Journal, 1987). The Amethyst vein of the Aquila prospect has estimated reserves of 30,000 t of ore grading 268 ppm Au and 940 ppm Ag (Wilson et al., 1988). Other less well explored areas may have undiscovered lodes of this type, such as those in the Mount Katmai quadrangle (Goldfarb et al., 1988).

Ore minerals include gold, galena, sphalerite, chalcopyrite, pyrite, marcasite, arsenopyrite, and native copper (Martin, 1905; Atwood, 1911; Wilson et al., 1988; White and Queen, 1989). Gangue minerals are quartz, sericite, calcite, and chlorite and locally, barite, clay, and rhodonite (Wilson et al., 1988); adularia is found in some of the Alaska-Apollo veins (White and Queen, 1989). At the Shumagin deposit, quartz veins are commonly open-space fillings with alternating layers of hydrothermal quartz and chlorite; galena and sphalerite are found in vugs or are associated with microscopic gold and chlorite. In some veins minor gold is associated with pyrite and marcasite (White and Queen, 1989). Ores from the Shumagin prospect have a Au-Ag-Te-Pb-Zn-Mn-Cu geochemical signature; wide As-Hg aureoles have been observed around some veins (White and Queen, 1989). In addition, heavy mineral concentrate samples collected from streams near the Alaska-Apollo deposit contain anomalously high concentrations of Ag, Pb, Zn, Au, and Sb (Frisken, 1992).

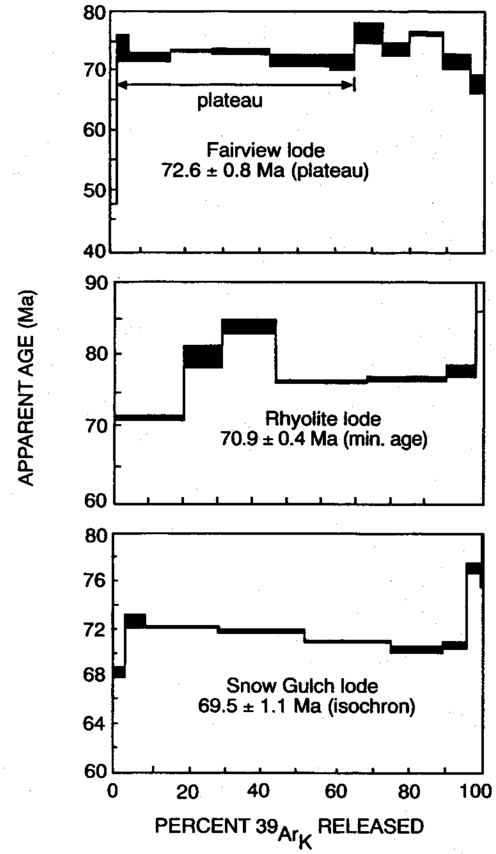

FIG. 5. Age spectra for hydrothermal sericite samples collecte selected Hg-Sb lodes dated by the $^{40}Ar/^{39}Ar$ technique.

Geochronology

Southwestern Alaska Hg-Sb lodes

Hydrothermal sericite is observed locally in some of the southwestern Alaska Hg-Sb lodes (Fig. 4). For this study, hydrothermal sericite was separated from altered rock zones adjacent to mineralized veins from the Fairview, Rhyolite, and Snow Gulch lodes. At all of these sites, mineralized veins are located in altered granite-porphyry dikes or adjacent sedimentary rocks of the Kuskokwim Group; sericite and kaolinite replace potassium feldspar in the altered dikes. Field and petrographic observations of intergrown cinnabar, stibnite, and hydrothermal sericite indicate that sericite formation and ore-mineral precipitation are coeval (Fig. 4). Rock samples containing sericite were crushed, pulverized, and sieved. Purified sericite separates were generally obtained by heavy liquid, magnetic, and paper-friction separations. Handpicking was necessary to obtain sericite samples with a purity of at least 99 percent.

Age determinations for the Hg-Sb vein lodes were made using the $^{40}Ar/^{39}Ar$ technique (Dallmeyer, 1975; Dalrymple et al., 1981), a variation of the conventional K/Ar method. A major advantage of the $^{40}Ar/^{39}Ar$ technique is that, for a single sample, a series of ages can be calculated for each of several progressively increasing temperature steps, usually 10 to 15 steps with the range of 400° to 1,500°C. Although argon loss or gain is commonly observed in the initial heating steps, an age spectrum is usually produced in the later heating steps, forming a plateau of ages (Fig. 5). Plateau ages are those where several successive heating steps have similar ages within analytical error and make up more than 50 percent of the total gas released. A plateau age, which represents the average age of the undisturbed portion of the age spectrum, is the best estimate of the time the sample closed to diffusion of argon (Snee et al., 1988). When plateau ages were not present in the data, the sample was considered disturbed and isochron or minimum ages were calculated instead.

Ages for southwestern Alaska Hg-Sb lodes are 72.6 ± 0.8 Ma (plateau age) for Fairview; ≥69.5 ± 1.1 Ma (isochron age) for Snow Gulch; and ≥70.9 Ma (minimum age) for Rhyolite (Fig. 5). These hydrothermal sericite ages overlap those of 75 to 56 Ma intrusions spatially associated with the lodes and indicate that there is a temporal relationship between Hg-Sb mineralization and Late Cretaceous and early Tertiary magmatism in southwestern Alaska.

Ages for two Unga Island gold-bearing vein lodes

Radiometric K/Ar ages have been determined for two vein lodes on Unga Island (Wilson et al., 1994). Adularia in a mineralized quartz vein from the Alaska-Apollo mine ± 0.5 Ma. A whole-rock sample collected at the Lake pect was dated at 31.3 ± 0.6 Ma; the sample was a volcanic rock pervasively altered to quartz and sericite that was probably originally an Oligocene volcanic rock. These two dates are similar to those of volcanic rocks that host gold vein lodes elsewhere in the region (Wilson et al., 1994). Although not many of the gold vein lodes in this area have been dated, similar ages for host rocks and lodes indicate that there is a temporal relationship between volcanism of the Meshik magmatic arc and formation of at least two of these lodes.

Fluid Inclusion Studies of Hg-Sb Lodes

Fluid inclusion studies were conducted on vein samples from several Hg-Sb lodes in southwestern Alaska to help constrain the nature of the ore-forming fluids and the environment of deposition. Microthermometry measurements and mass spectrometry analyses were made on fluid inclusions in hydrothermal quartz crystals containing cinnabar or on quartz crystals intergrown with cinnabar. Microthermometry measurements were made on doubly polished thin sections of vein samples using a modified U.S. Geological Survey gas-flow heating and cooling stage. Inclusions were frozen and then slowly heated to determine phase transitions such as ice-melting and homogenization temperatures. Homogenization temperatures for the fluid inclusions were determined when the vapor bubble disappeared and homogenized into the liquid phase. Analytical reproducibility is about ±0.2°C for ice-melting temperatures and about ±3°C for homogenization temperatures.

The fluid inclusions studied were a two-phase, liquid + vapor type. Daughter salt minerals were not observed in the fluid inclusions. Such liquid-vapor inclusions are common in many epithermal deposits (Bodnar et al., 1985). The inclusions observed were small, usually 1 to 10 μm in diameter, and were most commonly isolated inclusions along quartz crystal growth planes. The fluid inclusions studied were classified as primary, using the criteria described by Roedder (1979). Secondary inclusions were also observed but not studied. For the Red Devil, Decourcy Mountain, Kagati Lake, and Fairview lodes discussed here, fluid inclusion homogenization temperatures ranged from about 131° to 211°C (Fig. 6). Although some minor differences were observed in homogenization temperatures between lodes, these temperatures confirm the epithermal character of the Hg-Sb lodes studied. Ice melting temperatures indicate that fluid salinities vary from 1.5 to 4.6 wt percent NaCl equiv; such low salinities are similar to those observed in other epithermal deposits (Bodnar et al., 1985). In a fluid inclusion study of the Red Devil, Cinnabar Creek, Decourcy Mountain, and White Mountain mines, Belkin (1993) reports that 300 liquid + vapor inclusions in quartz associated with cinnabar yielded homogenization temperatures ranging from 135° to 226°C and salinities from 1 to 4 wt percent NaCl equiv; additionally, 50 liquid + vapor inclusions in cinnabar yielded homogenization temperatures from 160° to 190°C and salinities of about 3.5 wt percent NaCl equiv. Belkin (1993) also describes fluid inclusions in quartz crystals from the Cinnabar Creek deposit that contain pure CO_2 and CO_2 + H_2O and have hydrate-melting temperatures that indicate the presence of hydrocarbons. Similarly, Roedder (1963) observed three phase inclusions containing CO_2 liquid + H_2O liquid and CO_2 gas in quartz crystals from the Red Devil deposit. These results indicate that phase separation of H_2O and supercritical CO_2 occurred, at least locally, at the Red Devil and Cinnabar Creek deposits. Using trapping temperatures of about 130° to 210°C and assuming that confining pressure was hydrostatic, the resultant pressure-volume-temperature relationships indicate trapping pressures of about 150 to 200 bars, or a depth of formation for the Hg-Sb lodes of about 1,500 m (Miller et al., 1989). If the confining pressure was partially lithostatic (which is more realistic), then the depth of formation would be less than 1,500 m.

Microthermometry data and quadrupole mass spectrometric analysis of fluid inclusion volatiles (Landis and Hofstra, 1991) provide a quantitative estimate of the composition of the inclusions. Volatile compositions of fluid inclusions were determined for hydrothermal quartz crystals from Red Devil and Decourcy Mountain (Fig. 7). Microthermometry data indicate that the fluid inclusions generally contain more than 95 percent H_2O; gas analyses indicate that inclusions contain as much as about 4 percent CO_2, with traces of N_2 and CH_4.

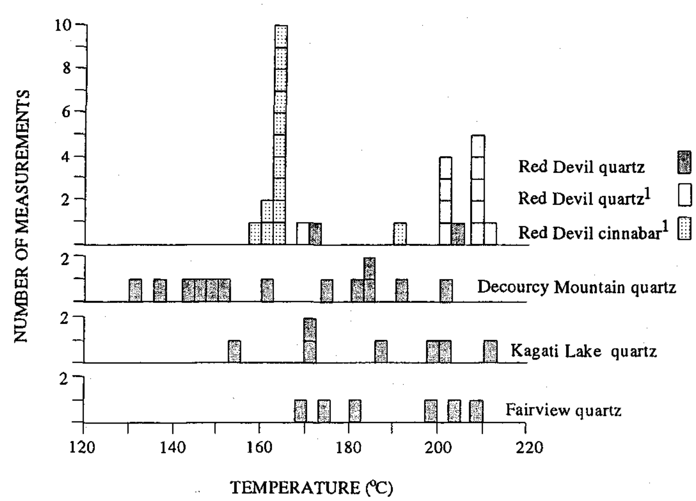

FIG. 6. Homogenization temperatures for fluid inclusions in cinnabar and quartz from southwestern Alaska Hg-Sb lodes. Data on Red Devil quartz and Red Devil cinnabar from Miller et al. (1989).

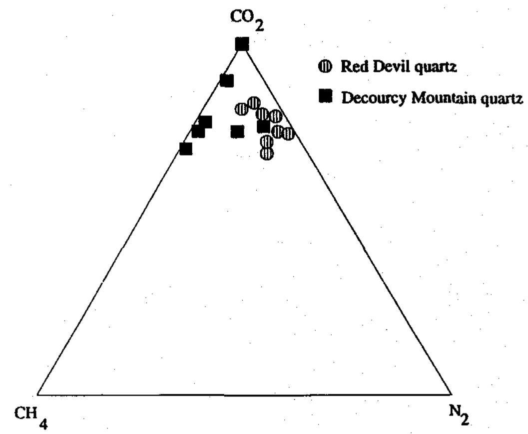

FIG. 7. Mass spectrometry data for CO_2, CH_4, and N_2 gases in fluid inclusions in samples collected from the Red Devil and Decourcy Mountain deposits.

These results confirm the presence of hydrocarbons in some fluid inclusions and indicate that organic matter was added to ore fluids during the formation of the Hg-Sb lodes. The most likely source of organic matter is local sedimentary rocks.

Isotopic Studies of Hg-Sb Lodes

Oxygen and hydrogen

Oxygen isotope ratios were measured in pure mineral separates, primarily in hydrothermal quartz associated with ore minerals; a few determinations were made on hydrothermal dickite and calcite (Table 3). Hydrogen isotope ratios were determined for dickite and one sericite sample. Isotopic ratios were determined using standard extractions and mass spectrometry techniques (Godfrey, 1962; Taylor and Epstein, 1962; Clayton and Mayeda, 1963; Savin and Epstein, 1970). Hydrogen ratios were normalized to Vienna-standard mean ocean water (V-SMOW) and standard light Antarctic precipitation. Analytical reproducibility is ± 0.2 per mil for oxygen and ± 3 per mil for hydrogen. Isotope values are expressed relative to V-SMOW in standard $\delta^{18}O$ notation for oxygen and in δD notation for hydrogen. The $\delta^{18}O$ values of hydrothermal fluids were calculated (Fig. 8) using formation temperatures obtained from fluid inclusion studies and equilibrium fractionation equations for quartz-water (Clayton et al., 1972), kaolinite-water (Kulla and Anderson, 1978), and calcite-water (O'Neil et al., 1969).

The $\delta^{18}O$ values for vein quartz from the southwestern Alaska Hg-Sb lodes are highly variable and range from 0.3 (Red Top) to 29.4 (Decourcy Mountain) per mil (Table 3). Using an average homogenization temperature (180°C) from fluid inclusion studies, the compositions of ore fluids calculated to be in equilibrium with hydrothermal quartz are highly variable, ranging from about −11 to +15 per mil $\delta^{18}O$ (Fig. 8). To evaluate any possible involvement of meteoric water in the formation of the Hg-Sb lodes, modeling calculations were made using the isotopic exchange equation for water-rock systems of Field and Fifarek (1985). Variables in these calculations included (1) the range of fluid inclusion homogenization temperatures (130°–210°C), (2) an isotopic composition of present-day meteoric water in southwestern Alaska of $\delta^{18}O = -20$ per mil and $\delta D = -150$ per mil, (3) the average oxygen isotope composition of wall rocks ($\delta^{18}O = 18$), and (4) water/rock ratios of 10, 1, 0.1, and 0.01. Using this approach, evolution paths of meteoric water were generated with varying water/rock ratios at 130°C and 210°C (Fig. 8). These calculations indicate that when meteoric water exchanges with surrounding sedimentary rocks at low water/rock ratios (0.01), it is possible to shift the final fluid $\delta^{18}O$ value to about 6 per mil at 210°C or to about 0.2 per mil at 130°C (Fig. 8). These are the heaviest $\delta^{18}O$ fluid values that can be obtained by isotopic exchange of meteoric water with wall rocks at these temperatures. However, most of the hydrothermal fluid $\delta^{18}O$ values for the southwestern Alaska Hg-Sb lodes have much heavier oxygen isotope compositions, plotting to the right of the meteoric water evolution curves (Fig. 8). Most of these ore fluids ranged from about 7 to 15 per mil $\delta^{18}O$, indicating that fluids that formed these lodes were derived largely from a heavy oxygen isotope source and that if meteoric water was involved, it was not the dominant fluid source. These water/rock calculations also indicate that lodes such as Red Top, Mountain Top, and Fisher Dome which have fluid compositions of less than 6 per mil were probably derived largely from oxygen isotope exchanged meteoric water.

Sedimentary rocks generally have high $\delta^{18}O$ values; for example, $\delta^{18}O$ values of clastic sedimentary rocks vary from about 8 to 25 per mil and those of chemical sedimentary rocks are as high as about 40 per mil (Taylor, 1979; Field and Fifarek, 1985; Longstaffe, 1987). Clastic sedimentary rocks generally retain the oxygen isotope characteristics of the source rocks from which they were derived, but weathering commonly produces ^{18}O-rich clay minerals with $\delta^{18}O$ values as high as about 30 per mil (Longstaffe, 1987). In addition, cements and chemical sediments are rich in ^{18}O because they have precipitated from fluids at low temperatures, resulting in high isotopic fractionations. As a result, clastic sedimentary rocks have oxygen isotope values between those of unaltered igneous source rocks ($\delta^{18}O$ = about 5–10‰) and clay minerals ($\delta^{18}O$ = 30‰; Longstaffe, 1987). The $\delta^{18}O$ values of whole-rock shale and graywacke samples of the Kuskokwim Group collected in this study range from 17.0 to 19.9 per mil, averaging about 18.2 per mil (Table 3), and are evidence of the presence of high $\delta^{18}O$ source rocks in the study area.

Oxygen isotope data indicate that hydrothermal fluids responsible for Hg-Sb deposition were derived from multiple sources. Meteoric water represents the light oxygen isotope reservoir, and sedimentary rocks spatially associated with the Hg-Sb lodes are a likely heavy oxygen isotope reservoir. Formation waters and hydrous minerals (mostly clays) in the sedimentary rocks would have about the same oxygen isotopic composition as the sedimentary rocks if they were in equilibrium. Hydrothermal fluids with isotopically heavy oxygen were probably generated when igneous intrusions heated the formation waters and dehydrated minerals in the surrounding sedimentary rocks. In such contact metamorphic zones, liberated hydrothermal fluids moved along fractures and, in some instances, mixed with local meteoric water. This interpretation is consistent with the close proximity of intrusions, sedimentary rocks, and the Hg-Sb lodes. Some contribution of magmatic water to the hydrothermal fluids, commonly $\delta^{18}O$ = 5 to 10 per mil (Taylor, 1979), may also have been possible, and is even likely, considering the close temporal and spatial relationship of the intrusions to the Hg-Sb lodes. Magmatic water cannot be the only heavy oxygen isotope reservoir, however, because it is not heavy enough isotopically to explain the high $\delta^{18}O$ fluid values for the Hg-Sb lodes.

Hydrogen isotope compositions (δD) of hydrothermal minerals (primarily dickite) from the Hg-Sb lodes are low, ranging from −92 to −181 per mil, and also indicate derivation of hydrogen from surrounding sedimentary rocks during dehydration. Constituents such as CO_2, CH_4, and N_2 are released during dehydration, devolatilization, oxidation, or exchange reactions in sedimentary rocks, forming organic-rich fluids or "organic waters" that are depleted in deuterium (Sheppard, 1986). The δD values for dickite from the southwestern Alaska Hg-Sb lodes plot within this organic water field (Fig. 8). Fluid inclusions containing CO_2, CH_4, and N_2 gases also suggest that they were added to ore fluids when sedimentary rock organic matter was broken down during the formation of the Hg-Sb lodes; another possibility is that these gases originated from local intrusions. The range of the δD values

TABLE 3. Summary of Isotopic Data for Hg-Sb Lodes and Rocks from Southwestern Alaska

Mine, lode, or sample type	$\delta^{18}O_{V\text{-}SMOW}$ quartz (or other minerals)	$\delta D_{V\text{-}SMOW}$	$\delta^{34}S_{CDT}$ Cinnabar	Stibnite	Other	$^{206}Pb/^{204}Pb$	$^{207}Pb/^{204}Pb$	$^{208}Pb/^{204}Pb$
1. Red Devil mine	19.1, 24.4, 27.4[1]	−140 (d), −127 (d)[1]	−3.7[1]	−4.2[1]		18.886	15.586	38.454 (st)
2. Cinnabar Creek mine	22.8[1]	−102 (d)	−5.2[1]					
3. Decourcy Mountain mine	13.5, 29.4[1], 21.8 (d)	−107 (d)	−4.5[1]	−4.0[1]		18.854	15.605	38.580 (st, cn)
4. Barometer mine	27.9	−94 (d)	−4.4	−5.6	−3.4 (p)			
5. Fairview	24.6[1], 12.2 (d)	−148 (d), −115 (s)	−3.4[1]	−3.7[1]		18.970	15.615	38.577 (st)
6. Fisher Dome lode	15.2, 14.6[1]	−123 (d)		−6.2[1]		18.833	15.569	38.439 (st)
7. Kagati Lake lode	20.9, 12.6[1]		−4.8	−9.3	−4.4 (r), −3.0 (o)[1]	18.752	15.542	38.226 (st, cn)
8. Kolmakof mine	19.8	−136 (d)	−1.7					
9. McGimsey lode	23.1			−9.9				
10. Millers lode	21.6		−4.0					
11. Mountain Top mine	15.2	−110 (d)	−16.5[1]					
12. Rainy Creek lode	24.3, 24.6[1]				−6.7 (r)[1]			
13. Rhyolite lode	18.4		−2.3			18.967	15.591	38.496 (cn)
14. Red Top mine	0.3, 0.7, 5.3 (cc)		−6.8					
15. Snow Gulch lode	24.9, 24.5[1]	−181 (d)		−25.0, −23.2[1]		18.961	15.616	38.649 (st)
16. White Mountain mine	23.4		6.0[1]			19.027	15.651	38.135 (cn)
17. Willis mine	26.2	−92 (d)	−4.6	−5.3				
18. Granite Creek lode	0.8			−5.6		18.869	15.616	38.509 (st)
ML02					−21.8 (wr)			
ML03 shale					−5.2 (wr)			
KR01 shale					−22.5 (wr)			
KR04 shale					−8.2 (wr)			
KR05					−15.1 (wr)			
KR06					−26.5 (wr)			
47B graywacke					−8.3 (wr)			
MC01 graywacke	19.9 (wr)							
RD03 graywacke	17.8 (wr)							
RD04 graywacke	17.8 (wr)							
RD08 graywacke	19.0 (wr)							
PM02 graywacke	18.2 (wr)							
PM03 graywacke	17.8 (wr)							
PM05 graywacke	17.9 (wr)							
RD03 shale	18.7 (wr)							
MC01 shale	17.4 (wr)							
RD04 shale	17.4 (wr)							
RD08 shale	17.0 (wr)							
PM02 shale	18.8 (wr)							
Plutons								
Beaver Mountains						18.976	15.640	38.692 (pf)
Chicken Mountain						18.888	15.605	38.461 (pf)
Black Creek stock						18.845	15.590	38.407 (pf)
Additional plutons[2]								
Cripple Mountains 71						19.026	15.592	38.586 (wr)[2]
Cripple Mountains 72						19.195	15.567	38.548 (wr)[2]
Cripple Mountains 74a						19.104	15.561	38.496 (wr)[2]
Cripple Mountains 74c						18.646	15.583	38.379 (wr)[2]
Cripple Mountains 75						18.946	15.557	38.504 (wr)[2]
Cripple Mountains 77						18.872	15.572	38.445 (wr)[2]
Crooked Mountain 49h						18.873	15.555	38.330 (wr)[2]
Crooked Mountain 49i						19.020	15.567	38.439 (wr)[2]
Mount Plummer 4						18.981	15.576	38.545 (wr)[2]
Mount Plummer 61						19.042	15.559	38.469 (wr)[2]
Canyonck 36a						19.071	15.586	38.483 (wr)[2]

All shale and graywacke samples are from the Kuskokwim Group

Abbreviations: cc = calcite, CDT = Canyon Diablo troilite, cn = cinnabar, d = dickite, o = orpiment, p = pyrite, pf = plagioclase feldspar, r = realgar, s = sericite, st = stibnite, V-SMOW = Vienna-Standard Mean Ocean Water, wr = whole rock

[1] Data from Goldfarb et al. (1990)

[2] Data provided by E. Moll-Stalcup (written commun., 1993)

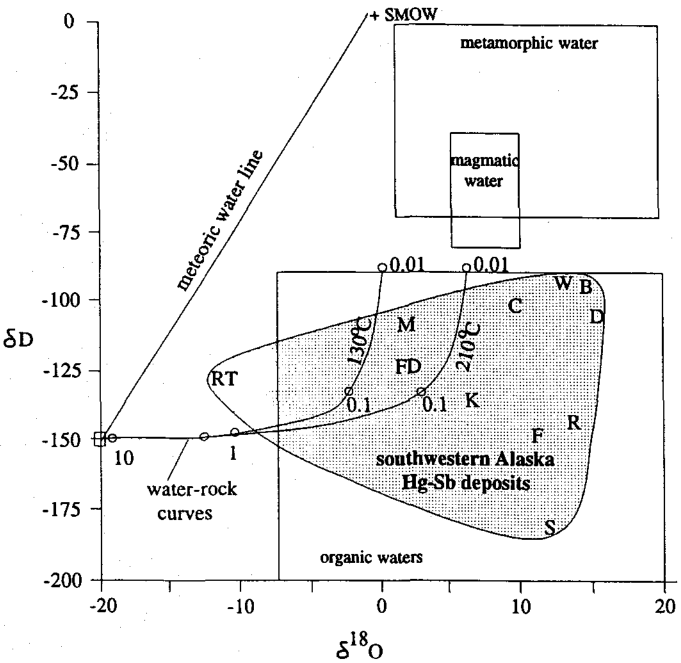

FIG. 8. Isotopic compositions of oxygen and hydrogen for ore fluids of the Hg-Sb lodes, calculated at 180°C using the fractionation equation of Clayton et al. (1972). Fields shown for reference are metamorphic and magmatic waters (Taylor, 1979) and organic waters (Sheppard, 1986). The water-rock curves were calculated at 130° and 210°C from the equation of Field and Fifarek (1985), showing water/rock ratios of 10, 1, 0.1, and 0.01. Abbreviations of Hg-Sb mines and lodes: B = Barometer mine, C = Cinnabar Creek mine, D = Decourcy Mountain mine, F = Fairview lode, FD = Fisher Dome lode, K = Kolmakof mine, M = Mountain Top mine, R = Red Devil mine, RT = Red Top mine, S = Snow Gulch lode, W = Willis mine.

in dickite indicates that some portion of the hydrogen was inherited from sedimentary rocks during breakdown of organic matter. Dehydration and devolatilization is the most likely mechanism for breaking down organic matter when the sedimentary rocks are heated during local intrusion of magmas.

Sulfur

Sulfur isotope ratios determined for mineral separates from ore samples and whole-rock samples of Kuskokwim Group rocks were used to identify sources of sulfur involved in the formation of the Hg-Sb lodes. The sulfide samples analyzed consisted of pure separates obtained by handpicking. Sulfur isotope measurements using mass spectrometry analysis followed procedures similar to those described by Grinenko (1962) and Yanaglsawa and Sakal (1983). Sulfur isotope ratios are expressed relative to Canyon Diablo troilite and have a precision of ±0.2 per mil.

The $\delta^{34}S$ data for samples of sulfide minerals from the Hg-Sb lodes indicate derivation of sulfur from multiple sources, such as local sedimentary rocks (−26.5 to −5.2‰ $\delta^{34}S$; Table 3) and magmatic sulfur (0 ± 3‰; Ohmoto and Rye, 1979). All of the $\delta^{34}S$ values for ore sulfides are between −25.0 and −1.7 per mil and are within the $\delta^{34}S$ endpoint values defined by local sedimentary rocks and magmatic sulfur, with the exception of a cinnabar sample (6.0‰) from the White Mountain mine. The negative $\delta^{34}S$ values determined for most of the sulfide minerals are similar to those for shale of the Kuskokwim Group (Fig. 9) and indicate that a signi[illegible] proportion of sulfur was probably derived from local sed[illegible]tary rocks during the formation of the Hg-Sb lodes. Neg[illegible] $\delta^{34}S$ values, similar to those of shale from the Kuskokwim Group, have been observed in modern organic-rich sediments and ancient sedimentary rocks; such isotopic characteristics probably result from isotopic fractionation during diagenetic sulfate reduction, forming pyrite and organic sulfur compounds (Ohmoto and Rye, 1979; Coleman and Raiswell, 1981). The negative $\delta^{34}S$ values for ore sulfides from the Hg-Sb lodes indicate derivation from a light sulfur source, probably sedimentary pyrite and organic sulfur leached from surrounding sedimentary rocks during formation of the Hg-Sb lodes.

Sulfides from some of the Hg-Sb lodes have heavier $\delta^{34}S$ compositions than those determined for samples of shale from the Kuskokwim Group (Fig. 9). About half of the ore sulfide minerals have $\delta^{34}S$ values between −1.7 and −5.2 per mil, and because the heaviest $\delta^{34}S$ value determined for the sedimentary rocks is −5.2 per mil, a heavier $\delta^{34}S$ source (such as that from magmatic sulfur) is required to explain the sulfide mineral $\delta^{34}S$ values. Assuming sulfide precipitation at 180°C and using isotopic fractionation equations for cinnabar-H_2S and stibnite-H_2S (Ohmoto and Rye, 1979), H_2S compositions would be about 3.5 per mil heavier for ore fluids calculated to be in equilibrium with these sulfide minerals. Calculated ore fluid $\delta^{34}S$ values therefore range from −21.6 per mil (Snow Gulch stibnite) to 9.1 per mil (White Mountain cinnabar), with most values ranging from −6.5 to −1.4 pe[illegible] This latter group is similar to magmatic sulfur isotope c[illegible]sitions. Magmatic sulfur averages about 0 ± 3 per m[illegible] though some crustally derived granites have anomalous $\delta^{34}S$ values greater than 10 per mil (Ohmoto and Rye, 1979). The close spatial association of intrusions and Hg-Sb lodes suggests that magmatic sulfur would be a possible component in the ore-forming fluids. A magmatic sulfur source could be derived from magmatic fluids or dissolution of sulfide minerals in the igneous rocks during hydrothermal alteration. In some lodes, ore is in pervasively altered igneous rocks, thereby making leaching of igneous sulfide minerals possible. The $\delta^{34}S$ values for cinnabar from lodes spatially associated with, or hosted by, granite-porphyry intrusions at Rhyolite (−2.3‰), Kolmakof (−1.7‰), and Fairview (−3.4‰) indicate derivation of sulfur from local igneous rocks.

Cinnabar from the White Mountain mine has the only

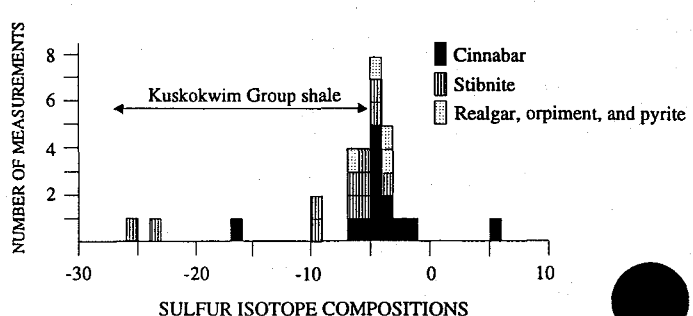

FIG. 9. Sulfur isotope compositions for ore minerals from the Hg-Sb lodes and surrounding sedimentary rocks.

positive $\delta^{34}S$ value (6‰) in the study. The White Mountain mine is also the only southwestern Alaska Hg-Sb deposit located primarily in carbonate rocks, and the isotopically heavy $\delta^{34}S$ value for cinnabar from the White Mountain mine suggests derivation of sulfur from sulfate minerals in the surrounding Ordovician marine carbonate rocks. The $\delta^{34}S$ values for seawater sulfate are age dependent and are about 25 to 30 per mil for Ordovician rocks (Claypool et al., 1980). When hydrothermal fluids reacted with sulfate minerals in the carbonate rock near White Mountain, the cinnabar that precipitated was isotopically lighter in sulfur than the rock sulfate. The degree of such isotopic fractionation depends on fluid chemistry, pH, oxygen fugacity, and other factors (Ohmoto and Rye, 1979). One should add that the possibility of a local source of magmatic sulfur cannot be discounted, because Late Cretaceous and early Tertiary dikes cut carbonate rocks of the Holitna Group near the White Mountain mine.

Lead

Isotopic compositions of lead in ore minerals were used to determine the sources of lead involved during the formation of the Hg-Sb lodes. Lead isotope compositions were measured in ore mineral separates from vein samples (Table 3). All lead isotope determinations were made by solid-source mass spectrometry. Values were corrected for thermal fractionation using the NBS SRM-981 common lead standard and are accurate within 0.1 percent at the 95 percent confidence level (Church et al., 1987).

The lead isotope compositions of ores from the Hg-Sb lodes (Fig. 10) range from $^{206}Pb/^{204}Pb$ = 18.75 to 19.03, $^{207}Pb/^{204}Pb$ = 15.54 to 15.65, and $^{208}Pb/^{204}Pb$ = 38.14 to 38.65. These data are interpreted in reference to the plumbotectonics model (Doe and Zartman, 1979) that defines the lead isotope characteristics of geologic environments, or reservoirs, such as mantle, lower crust, continental crust, and the orogen. The orogen is a mixing curve with contributions from the upper crust, lower crust, and mantle that approximates compositions of island- and continental-arc rocks. The lead isotope compositions from the Hg-Sb lodes define a mixing array that plots near the endpoint composition of the orogen curve on the uranogenic diagram (^{207}Pb-^{206}Pb) and overlaps the upper crust curve on the thorogenic diagram (^{208}Pb-^{206}Pb). The lead isotope compositions of the Hg-Sb lodes are similar to those of Late Cretaceous and early Tertiary igneous rocks in southwestern Alaska (Szumigala, 1993; E. Moll-Stalcup, written commun., 1995). The majority of the data from the Hg-Sb lodes also overlap with lead isotope compositions of ore deposits in Mesozoic and Cenozoic sedimentary rocks and continental-arc rocks (Doe and Zartman, 1979). The lead isotope composition of the Hg-Sb lodes indicates derivation of lead from multiple sources, such as upper crustal sedimentary rocks and magmatic arc rocks, which is consistent with the local geology of the lodes. The range in lead isotope compositions of the Hg-Sb ores represents the heterogeneity within surrounding sedimentary and igneous rocks and indicates leaching of lead, and perhaps other metals, from these rocks. The radiogenic character of lead isotope values of the Hg-Sb lodes indicates that any involvement of lead from a mantle source was probably minor; for example, local intrusions spatially associated with the Hg-Sb lodes may provide a source of mantle lead because they were formed in a magmatic arc. The lead isotope data for the Hg-Sb lodes indicate little or no lead from a lower crust (cratonized crust) source.

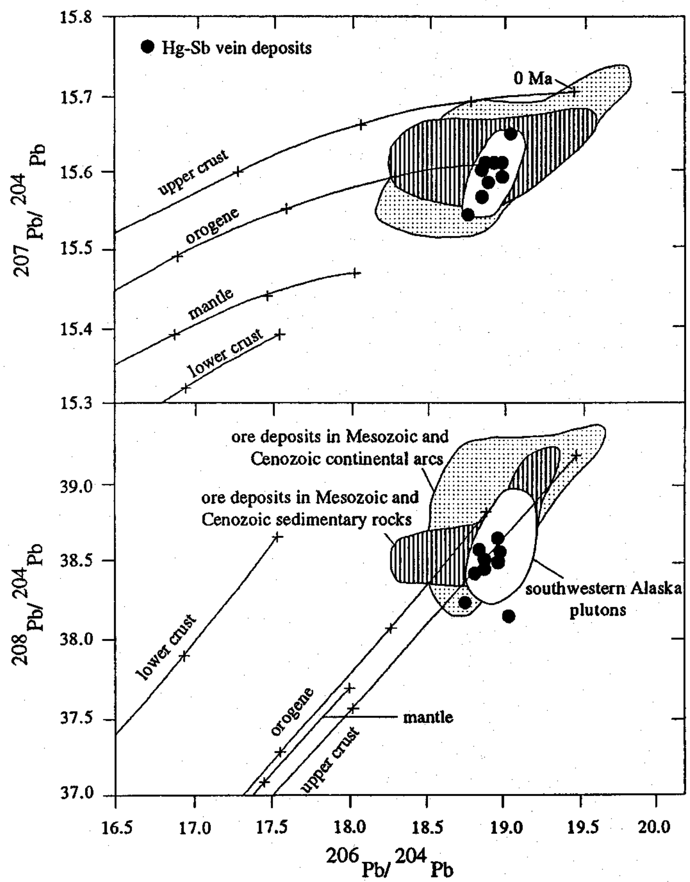

FIG. 10. Pb isotope compositions of ores from southwestern Alaska Hg-Sb lodes compared to those of the mantle, upper crust, lower crust, and orogen curves from the plumbotectonics model of Doe and Zartman (1979). The orogen is a mixing curve using components from the mantle, upper crust, and lower crust environments that is modeled to represent island and continental arcs. Marks (+) on the curves indicate 400-m.y. intervals. Fields for ore deposits of Cenozoic and Mesozoic age were generalized from Doe and Zartman (1979).

Cinnabar from the White Mountain mine has a lead isotope composition that differs from the majority of the Hg-Sb deposits. Cinnabar from the White Mountain mine has a lower $^{208}Pb/^{204}Pb$ ratio than the other ores, but it is the only southwestern Alaska Hg-Sb deposit found predominantly in carbonate rocks. The depleted $^{208}Pb/^{204}Pb$ composition of ore from the White Mountain mine indicates that lead derived from thorium (^{208}Pb) is depleted in these carbonate rocks.

Discussion

Hg-Sb lodes

Using the classification of Lindgren (1933), the southwestern Alaska Hg-Sb lodes are considered epithermal hydrothermal deposits. Diagnostic characteristics of these lodes include their Hg-Sb-As geochemistry, formation temperatures of about 200°C, quartz and carbonate gangue, argillic alteration, mineralized forms including veins, vein breccias, stockworks, replacements, disseminations, and open-space ore textures.

Many of these characteristics are similar to those of hot spring mercury deposits (White and Roberson, 1962; White, 1967; Rytuba, 1986). Perhaps the best example of an epithermal hot spring system is McLaughlin, California, where cinnabar in siliceous sinter (the Manhattan mine) was located above a gold-rich deposit (the McLaughlin mine; Lehrman, 1986; Gustafson, 1991). Siliceous sinter representing surface deposition of silica that is common in hot spring deposits has not been observed in any of the southwestern Alaska Hg-Sb lodes, but erosion could have removed any sinter deposits. The southwestern Alaska Hg-Sb lodes commonly consist of mineralized veins and vein breccias that formed below the surface in shallow environments, similarly to other epithermal deposits (Buchanan, 1981).

The southwestern Alaska Hg-Sb lodes are considered to be analogues of the northern California mercury deposits. Mercury deposits in California have been extensively studied; examples include Sulphur Bank (White and Roberson, 1962; Wells and Ghiorso, 1988; Donnelly-Nolan et al., 1993), New Idria (Boctor et al., 1987), McLaughlin and Manhattan (Lehrman, 1986; Gustafson, 1991; Sherlock and Jowett, 1992), Culver-Baer (Peabody and Einaudi, 1992), and the Wilbur Springs district (Donnelly-Nolan et al., 1993). For most of these deposits, geologic, isotopic, and age data indicate that there is a relationship between mercury mineralization and the heating of sedimentary rocks in response to magmatism (White and Roberson, 1962; White et al., 1973; Peabody and Einaudi, 1992; Donnelly-Nolan et al., 1993). Isotopic and fluid chemistry characteristics of several of the northern California deposits indicate that ore fluids were derived primarily from mixed evolved connate and meteoric waters (White, 1957; White et al., 1973; Donnelly-Nolan et al., 1993). Donnelly-Nolan et al. (1993) related hydrothermal activity to shallow magmatism that heated sedimentary and metasedimentary rocks of the Franciscan Complex and Great Valley sequence and initiated thermal convection and hydrothermal fluid flow along fractures and faults, primarily the San Andreas transform fault system. It is likely that organic material from sedimentary rocks was contributed to local fluids during hydrothermal activity. Organic carbon was interpreted as a source for CO_2 in the Culver-Baer mercury deposit (Peabody and Einaudi, 1992).

Geologic, fluid inclusion, and isotopic data for the southwestern Alaska Hg-Sb lodes presented in this study indicate that ore fluids were derived from multiple sources. Most of the ore fluids probably originated from sedimentary rocks, but evolved meteoric water and magmatic water were important fluid sources for some lodes. The majority of the lodes studied have heavy oxygen isotope ore fluid compositions ($\delta^{18}O$) of about 6 to 15 per mil, which indicate a sedimentary rock source. Light sulfur and hydrogen isotope compositions of the Hg-Sb lodes also indicate derivation from sedimentary rocks. Hydrous minerals and formation waters were the fluid sources in the sedimentary rocks. Because these rocks have undergone little or no regional metamorphism (Miller et al., 1989), there has been only minor dewatering of the rocks and the clay minerals have not undergone conversion to metamorphic minerals. Hydrous minerals, formational waters, and sedimentary rocks would have similar $\delta^{18}O$ compositions, because the trapped waters gradually equilibrate isotopically with the rocks over time. Some of the Hg-Sb lodes have $\delta^{18}O$ fluid compositions as low as −11 per mil; such light values are interpreted to represent ev meteoric water. Thus, the dominant fluid sources were sedimentary rocks and meteoric waters, though some component of magmatic water with $\delta^{18}O$ values of about 5 to 10 per mil is also possible and consistent with the geology of the lodes. In addition, $\delta^{34}S$ values of ore sulfide minerals indicate that sulfur was derived from sedimentary rock and magmatic sources during the formation of the Hg-Sb deposits.

The close spatial association and similar ages of the Hg-Sb lodes and intrusions indicate a relationship between mineralization and magmatism (Fig. 11). High heat flow related to igneous activity probably induced dehydration in contact metamorphic zones in the sedimentary rocks. The igneous activity initiated thermal convection, expelled formation waters, and dehydrated minerals from contact metamorphic aureoles. These expelled hydrothermal fluids flowed through fractures, reacted with wall rocks, and in some cases mixed with meteoric water. The presence of solid and liquid hydrocarbons in some of the Hg-Sb lodes and the occurrence of fluid inclusions containing constituents such as CO_2, N_2, and CH_4 probably indicate that organic matter in the sedimentary

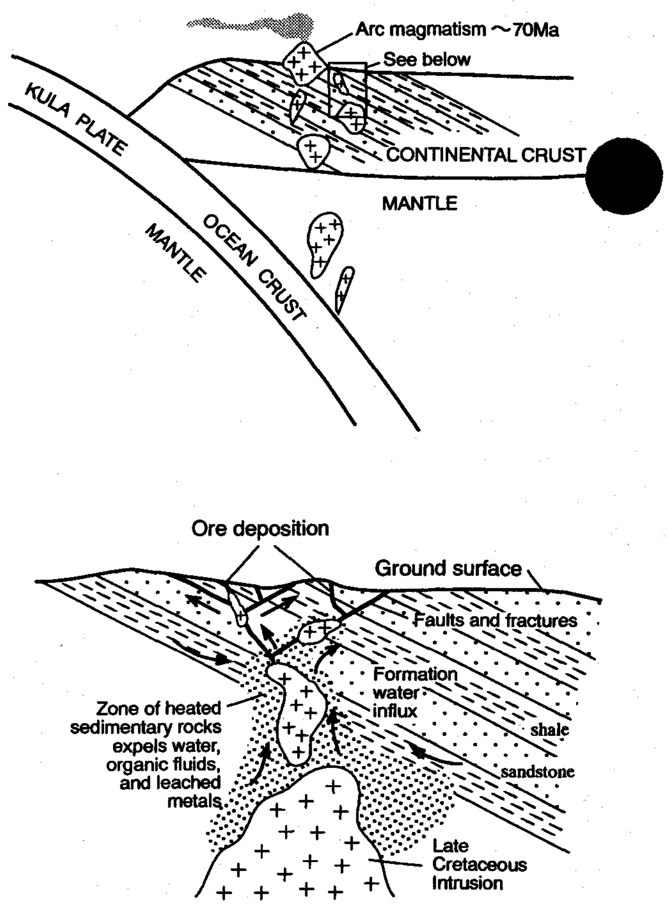

FIG. 11. Schematic formation model for the southwestern Alaska Hg-Sb lodes. Hydrothermal activity is closely related to emplacement magmas into mostly intercalated shales and sandstones. Fluids are e from the heated sedimentary rocks and flow along faults and fractures, ing vein lodes near the surface. Arrows indicate direction of hydrothermal fluid flow.

rocks was also broken down during contact metamorphism and released into ore fluids.

In addition to organic compounds, mercury was probably also derived from local sedimentary rocks. Average mercury and antimony concentrations are typically higher in shale (0.4 ppm Hg, 2 ppm Sb) than in felsic (0.08 ppm Hg, 0.26 ppm Sb), mafic (0.09 ppm Hg, 1 ppm Sb), and ultramafic (0.01 ppm Hg, 0.1 ppm Sb) igneous rocks (Govett, 1983). Average concentrations in samples of shale of the Kuskokwim Group are about 0.6 ppm Hg and 1.5 ppm Sb and are similar to worldwide averages (Table 4). These data indicate that wall-rock shale was an important local source of Hg and Sb. High metal concentrations in organic-rich sedimentary rocks indicate that organic matter may be important for complexing metals, especially mercury (Krupp, 1988). If the sedimentary rocks are the source of mercury, then there must be a process to mobilize and deposit the mercury. Magmatic intrusions probably provided enough heat to initiate the flow of hydrothermal fluid and the leaching of mercury-bearing sedimentary rocks. Krupp (1988) demonstrated that when sedimentary rocks with high mercury contents are heated, mercury can be transported as several complexes. Krupp (1988) also suggested that intercalated shale and sandstone make better source rocks, because even though shale may have a higher mercury content, sandstone has greater permeability, which enhances fluid flow through such rocks as well as along local fractures.

Several studies have indicated that mercury in hydrothermal fluids is most likely to be transported as $Hg^{o}_{(g)}$, $Hg^{o}_{(aq)}$, as mercury bisulfide complexes, or as organic complexes (Barnes, 1979; Varekamp and Buseck, 1984; Krupp, 1988). When vapor is present, mercury partitions strongly into the vapor phase (Varekamp and Buseck, 1984). Vapor-phase transport of mercury is likely to result above 200°C (Barnes, 1979) but is also possible below 100°C (White, 1967). It is uncertain which transporting mechanism was most important in the southwestern Alaska lodes. However, mineral relationships in the Alaskan lodes generally show cinnabar intergrown with other ore minerals, most commonly stibnite (and occasionally gold), which would argue against the vapor transport of mercury. The majority of mercury transport was probably as an aqueous phase, though mercury vapor transport may have resulted locally, because ore containing only cinnabar is found in some lodes.

For the southwestern Alaska Hg-Sb lodes, cinnabar, and perhaps stibnite, deposition most likely resulted from oxidation or cooling. In addition, hydrothermal fluid mixing with oxygenated meteoric waters may have been the mechanism for cinnabar precipitation in some of the Hg-Sb lodes studied, based on isotopic arguments; cooling, oxidation, or mixing of hydrothermal fluids would all have been possible as fluids approached the surface. Oxidation of ore fluid is the most efficient mechanism for precipitating cinnabar from the elemental state or mercury bisulfide complexes, commonly by mixing with oxygenated ground waters, and explains the common occurrence of cinnabar in shallow depositional environments (Barnes et al., 1967; Krupp, 1988; Wells and Ghiorso, 1988). Antimony in low-temperature hydrothermal systems is usually transported as an aqueous species (even during boiling), and precipitation of antimony sulfide minerals is strongly driven by a decrease in temperature or pH or by the addition of sulfide (Spycher and Reed, 1989). Stibnite deposition, like that of cinnabar, may have resulted as hydrothermal solutions (1) reached the surface and cooled, (2) boiled, effectively decreasing the pH of the solution, or (3) reacted with the surrounding sedimentary rocks that provided reduced sulfur.

TABLE 4. Average Hg and Sb Concentrations in Shale and Sandstone

Shale		Sandstone		
Hg	Sb	Hg	Sb	References
[24]0.62	[40]1.5	[43]0.36	[41]0.77	This study (all samples from the Kuskokwim Group)
0.02–0.4	1–2	0.03	1.0	Rose et al. (1979)
0.4	2	ND	ND	Govett (1983)

Concentrations in ppm; superscripts indicate number of determinations
ND = not determined

Gold associated with the Hg-Sb lodes

Ore samples collected from some southwestern Alaska epithermal Hg-Sb lodes contain anomalous concentrations of gold (Table 2). In addition, native gold was identified in heavy mineral separates of crushed ore from the Kolmakof and Red Devil mines. These results are not particularly unusual in that other epithermal mercury deposits are known to contain gold—for example, deposits such as the McLaughlin mine (Lehrman, 1986) and the Wilbur Springs district in California (Pearcy and Peterson, 1990; Donnelly-Nolan et al., 1993). Gold lodes may be present below some of the southwestern Alaska Hg-Sb lodes because, as mentioned previously, the epithermal Hg-Sb lodes are scattered throughout a broad region in which precious metal and base metal lodes are spatially related to Late Cretaceous and early Tertiary igneous complexes (Bundtzen and Miller, 1997). In addition, some of the precious metal lodes contain cinnabar (Bundtzen and Miller, 1997), which also indicates a possible association with the shallower mercury lodes. The epithermal Hg-Sb lodes in southwestern Alaska may represent shallow expressions of the deeper precious and base metal lodes.

The presence or absence of significant gold below the Hg-Sb lodes depends on a number of factors, including the thermal gradient of the hydrothermal system and the lateral and vertical extent of veining. Fluid inclusion formation temperatures for the southwestern Alaska Hg-Sb lodes are about 130° to 210°C; such low ore fluid temperatures appear to hinder gold mobility, because the solubility of gold bisulfide decreases sharply between 300° and 200°C (Seward, 1984). Assuming that, at some depth below the Hg-Sb lodes, ore fluids were hot enough to have transported gold, probably as a bisulfide complex (Romberger, 1988), much of the gold would have been precipitated from the fluids before they reached the low-temperature, near-surface environment. The relationship of gold to the Hg-Sb lodes has not been thoroughly investigated, but drilling data may help to determine gold grades and the lateral and vertical extent of gold.

Comparison of the southwestern Alaska Hg-Sb lodes to worldwide mercury belts

Mercury deposits worldwide are generally epithermal (<250°C) and formed in hydrothermal systems at shallow depths. Most of them are closely associated with two broad subduction-related volcanic-orogenic belts along present or past plate boundaries, the Hercynian belt extending through Asia and Europe and the circum-Pacific belt (Bailey, 1989). The Asian-European belt extends from northeastern Siberia through Russia, Mongolia, and China and west through the Himalayas into Turkey, Slovenia (Yugoslavia), Italy, Algeria, and Spain; this belt includes the three largest mercury deposits in the world, Almaden (Spain), Idria (Slovenia), and Monte Amiata (Italy). The circum-Pacific belt, which extends northward along the western margin of South, Central, and North America, across the Alaskan Aleutian Islands, then southward to Japan, the Philippines, and New Zealand (Bailey, 1989), includes major mercury deposits, such as those in the California Coast Ranges and Huancavelica, Peru. The Hg-Sb lodes in southwestern Alaska are part of the circum-Pacific belt.

Compared to other mercury deposits in the United States and throughout the world, the southwestern Alaska mercury mines are small. For example, the New Almaden mine in California has alone produced over 1,000,000 flasks of mercury, and the combined mercury production from mines in the state exceeds 3,500,000 flasks (Peabody, 1993). The largest mercury districts in the world are Almaden, Spain (with production of 7,500,000 flasks), Idria, Slovenia (3,000,000 flasks), Monte Amiata, Italy (2,000,000 flasks), and Huancavelica, Peru (1,500,000 flasks; Bailey et al., 1973; Peabody, 1993). Although the Alaskan lodes are small (with a total production of about 41,000 flasks) on a national and international scale, they have been historically important locally, providing mercury primarily for use in the Alaskan gold mining industry.

Mercury deposits are found in nearly all rock types, but studies of large mercury deposits such as Almaden, Spain (Rytuba et al., 1989; Saupé and Arnold, 1992), Huancavelica, Peru (McKee et al., 1986), and those in California (Donnelly-Nolan et al., 1993; Peabody, 1993) generally indicate that mercury deposit formation was related to interaction of igneous activity with surrounding rocks. Similarly, the southwestern Alaska Hg-Sb lodes are closely associated with igneous activity. The association was proposed by early studies, most notably those by Cady et al. (1955), that suggested a connection of lode formation and igneous activity based on geologic observations. However, Sainsbury and MacKevett (1965) suggested that the Hg-Sb lodes were generally contained in the igneous rocks and were therefore younger than the igneous activity and not directly related to the igneous rocks. Goldfarb et al. (1990) suggested the possibility of Hg-Sb lode formation from fluids expelled during burial metamorphism or contact metamorphism related to local igneous activity. The data presented in this study strongly favor a connection between Hg-Sb mineralization and subduction-related igneous activity indicating that ore fluids were derived primarily from surrounding sedimentary rocks as they were heated by local intrusions.

Gold-bearing vein lodes

Gold-bearing vein lodes of the Alaska Peninsula and Aleutian Islands are similar to volcanic-hosted epithermal adularia-sericite mineral deposits (Hayba et al., 1985). Diagnostic characteristics of the Alaska lodes include sericitic to argillic alteration with some adularia and propylitic alteration, strong structural control in a volcanic environment, predominantly andesitic host rocks, similar ages for host rocks and mineralization, and base metal sulfide and native gold minerals. These epithermal lodes are situated in rocks of a magmatic arc. Many of these lodes are spatially associated with Tertiary porphyry copper deposits that generally parallel the arc. Epithermal precious and base metal lodes are found in other magmatic-arc settings above porphyry systems, indicating a spatial and genetic association between the two deposit types (Sillitoe, 1991). Some of these porphyry deposits contain significant amounts of gold (Sillitoe, 1979). Tertiary epithermal gold-bearing vein lodes on the Alaska Peninsula and Aleutian Islands may also be genetically associated with porphyry deposits at depth (Wilson and Cox, 1983; Young et al., 1997). Strong structural control of gold-bearing vein lodes may indicate that faults and fractures in the magmatic arc provided a pathway for deep circulation of hydrothermal fluids, possibly connected to porphyry systems. A genetic link between these two deposit types in southwestern Alaska is uncertain, however, owing to limited ages and lack of isotopic data for the epithermal gold-bearing vein systems.

Additional discoveries of gold-bearing vein lodes in southwestern Alaska seem probable. Similar to the Hg-Sb lodes, gold vein lodes on the Alaska Peninsula and Aleutian Islands are found in remote areas where rocks are poorly exposed. High operating costs have hindered development of known occurrences. Recent studies indicate that many additional areas remain to be thoroughly evaluated for precious metal lodes (Wilson et al., 1996).

Summary

The southwestern Alaska epithermal Hg-Sb vein lodes are similar in age to the spatially associated intrusions, indicating that there is a temporal relationship between arc magmatism and mineralization. Ages for Hg-Sb lodes and nearby intrusions indicate that hydrothermal mineralization was closely related to the onset of Late Cretaceous-early Tertiary magmatism (about 75–56 Ma) generated during subduction of the Kula plate under southern Alaska (Moll-Stalcup, 1994). Geologic and isotopic data for the Hg-Sb lodes indicate that igneous activity provided the heat source to initiate hydrothermal convection and fluid flow. Ore fluids were derived from multiple sources, the primary one being sedimentary rocks heated by the local intrusion of magmas. This intrusion of magmas initiated dehydration reactions and expelled formation waters and organic fluids from the sedimentary rocks. Isotopically light oxygen ore fluid values indicate the involvement of exchanged meteoric water during the formation of some Hg-Sb lodes. Minor contributions of magmatic water to ore fluids are also possible and consistent with local geology. Local, organic-rich shale is the most likely source of mercury. Gold concentrations in samples of mineralized veins indicate that gold deposits may be possible below some of the southwestern Alaska Hg-Sb lodes. It is likely that additional Hg-Sb lodes will be discovered in southwestern Alaska, because (1) the terrain is generally low rolling where rocks are poorly exposed, owing to cover with vegetation and tundra, (2) the geology is conducive to additional discoveries (although most known lodes are located along the Kuskokwim River or other watersheds, indicating the need for additional exploration in the more remote interior), and (3) recent studies have identified significant mercury anomalies in stream sediment and heavy mineral concentrate samples collected in areas that have not been thoroughly investigated (Gray et al., 1993).

Existing data are too limited to allow development of a formation model for the epithermal gold-bearing vein lodes on the Alaska Peninsula and Aleutian Islands. Geologic, geochemical, and mineralogical characteristics of the lodes are similar to those of volcanic-hosted adularia-sericite epithermal vein deposits. The gold-bearing vein lodes are associated with Tertiary magmatism of the Meshik subduction arc. Ages for two of the lodes are closely related to those of host volcanic rocks of Oligocene age of the magmatic arc. These epithermal gold-bearing vein lodes may represent shallow expressions of deeper, arc-related porphyry systems.

Acknowledgments

Many of the ideas presented in this paper were developed through helpful discussions with T. Bundtzen (State of Alaska), D. Goldfarb, E. Moll-Stalcup, and J. Rytuba (U.S. Geological Survey). We thank R. O'Leary, J. Motooka, and B. Vaughn (U.S. Geological Survey) for chemical and isotopic analyses. P. Theodorakos and C. Borden (U.S. Geological Survey) assisted with fieldwork. We also thank J. McAtee and R. Retherford of the Calista Corporation for allowing access to their lands and for cooperative discussions. This paper was improved by technical reviews from K. Kelley and I. Ridley (U.S. Geological Survey) and two *Economic Geology* referees.

REFERENCES

Atwood, W.W., 1911, Geology and mineral resources of parts of the Alaska Peninsula: U.S. Geological Survey Bulletin 467, 137 p.

Bailey, E.H., 1989, Mercury resources, *in* Carr, D.D., and Herz, N., eds., Concise encyclopedia of mineral resources: Oxford, England, Pergamon Press, p. 197–198.

Barnes, H.L., 1979, Solubility of ore minerals, *in* Barnes, H.L., ed., Geochemistry of hydrothermal ore deposits, 2nd ed.: New York, John Wiley, p. 404–460.

Barnes, H.L., Romberger, S.B., and Stemprok, M., 1967, Ore solution chemistry, 2. Solubility of HgS in sulfide solutions: ECONOMIC GEOLOGY, v. 62, p. 957–982.

Belkin, H.E., 1993, Fluid inclusion systematics of epithermal mercury-antimony mineralization, southwestern Alaska, USA [abs.]: European Current Research on Fluid Inclusions Biennial Symposium, 12th, Warsaw and Cracow, Poland, June 13–18, 1993, Abstracts, p. 25–26.

Blodgett, R.B., and Clough, J.G., 1985, The Nixon Fork terrane: Part of an in place peninsular extension of the North American Paleozoic continent [abs.]: Geological Society of America Abstracts with Programs, v. 17, p. 342.

Boctor, N.Z., Shieh, Y.N., and Kullerud, G., 1987, Mercury ores from the New Idria district, California: Geochemical and stable isotope studies: Geochimica et Cosmochimica Acta, v. 51, p. 1705–1715.

Bodnar, R.J., Reynolds, T.J., and Kuehn, C.A., 1985, Fluid inclusion systematics in epithermal systems: Reviews in Economic Geology, v. 2, p. 73–97.

Box, S.E., 1985, Terrane analysis, northern Bristol Bay region, southwestern Alaska: Development of a Mesozoic interoceanic arc and its collision with North America: Unpublished Ph.D. dissertation, Santa Cruz, California, University of California, 163 p.

Box, S.E., and Elder, W.P., 1992, Depositional and biostratigraphic framework of the Upper Cretaceous Kuskokwim Group, southwest Alaska: U.S. Geological Survey Bulletin 1999, p. 8–16.

Box, S.E., Moll-Stalcup, E.J., Frost, T.P., and Murphy, J.M., 1993, Preliminary geologic map of the Bethel and southern Russian Mission quadrangles, southwestern Alaska: U.S. Geological Survey Miscellaneous Field Studies Map MF-2226-A, scale 1:250,000, 20 p.

Brown, F.R., 1947, Apollo mine (Unga Island): Alaska Territorial Department of Mines Miscellaneous Report MR 138–1, 33 p.

Buchanan, L.J., 1981, Precious metal deposits associated with volcanic environments in the southwest: Arizona Geological Society Digest, v. 14, p. 237–262.

Bundtzen, T.K., and Gilbert, W.G., 1983, Outline of geology and mineral resources of upper Kuskokwim region, Alaska: Alaska Geological Society Symposium, Anchorage, 1982, Proceedings, p. 101–117.

Bundtzen, T.K., and Miller, M.L., 1997, Precious metals associated with Late Cretaceous-early Tertiary igneous rocks of southwestern Alaska: ECONOMIC GEOLOGY MONOGRAPH 9, p. 242–286.

Bundtzen, T.K., Laird, G.M., Harris, E.E., Kline, J.T., and Miller, M.L., 1993, Geologic map and data file tables of the Sleetmute C-7, D-7, C-8, and D-8 quadrangles, Horn Mountains area, southwestern Alaska: Alaska Division of Geological and Geophysical Surveys Public-Data File 93–47, scale 1:63,360.

Burk, C.A., 1965, Geology of the Alaska Peninsula: Island arc and continental margin: Geological Society of America Memoir 99, 250 p.

Cady, W.M., Wallace, R.E., Hoare, J.M., and Webber, E.J., 1955, The central Kuskokwim region, Alaska: U.S. Geological Survey Professional Paper 268, 132 p.

Christie, J.S., 1974, Aleut-Quintana-Duval 1974 joint venture: Final report: Anchorage, Alaska, The Aleut Corporation, unpublished report, 24 p.

Church, S.E., Delevaux, M.H., and Gray, J.E., 1987, Pb-isotope database for sulfides from Alaska: U.S. Geological Survey Open-File Report 87–259, 44 p.

Claypool, G.E., Holser, W.T., Kaplan, I.R., Sakai, H., and Zak, I., 1980, The age curves of sulfur and oxygen isotopes in marine sulfate and their mutual interpretation: Chemical Geology, v. 28, p. 199–260.

Clayton, R.N., and Mayeda, T.K., 1963, The use of bromine pentafluoride in the extraction of oxygen from oxides and silicates for isotopic analyses: Geochimica et Cosmochimica Acta, v. 27, p. 43–52.

Clayton, R.N., O'Neil, J.R., and Mayeda, T.K., 1972, Oxygen isotope exchange between quartz and water: Journal of Geophysical Research, v. 77, p. 3057–3067.

Coleman, M.L., and Raiswell, R., 1981, Carbon, oxygen, and sulphur isotope variations in concretions from the Upper Lias of N.E. England: Geochimica et Cosmochimica Acta, v. 45, p. 329–340.

Collier, A.J., 1905, Auriferous quartz veins on Unalaska Island: U.S. Geological Survey Bulletin 259, p. 102–103.

Dallmeyer, R.D., 1975, Incremental $^{40}Ar/^{39}Ar$ ages of biotite and hornblende from retrograded basement gneisses of the southern Blue Ridge: Their bearing on the age of Paleozoic metamorphism: American Journal of Science, v. 275, p. 444–460.

Dalrymple, G.B., Alexander, E.C., Lanphere, M.A., and Kraker, G.P., 1981, Irradiation of samples for $^{40}Ar/^{39}Ar$ dating using the Geological Survey TRIGA reactor: U.S. Geological Survey Professional Paper 1176, 56 p.

Decker, J., and Hoare, J.M., 1982, Sedimentology of the Cretaceous Kuskokwim Group, southwest Alaska: U.S. Geological Survey Circular 844, p. 81–83.

Decker, J., Bergman, S.C., Blodgett, R.B., Box, S.E., Bundtzen, T.K., Clough, J.G., Coonrad, W.L., Gilbert, W.G., Miller, M.L., Murphy, J.M., Robinson, M.S., and Wallace, W.K., 1994, Geology of southwestern Alaska: Boulder, Colorado, Geological Society of America, Geology of North America, v. G1, p. 285–310.

Decker, J., Reifenstuhl, R.R., Robinson, M.S., Waythomas, C.F., and Clough, J.G., 1995, Geology of the Sleetmute A-5, A-6, B-5, and B-6 quadrangles, southwestern Alaska: Alaska Division of Geological and Geophysical Surveys Professional Report 99, 16 p.

Doe, B.R., and Zartman, R.E., 1979, Plumbotectonics, the Phanerozoic, *in* Barnes, H.L., ed., Geochemistry of hydrothermal ore deposits, 2nd ed.: New York, John Wiley, p. 22–70.

Donnelly-Nolan, J.M., Burns, M.G., Goff, F.E., Peters, E.K., and Thompson, J.M., 1993, The Geysers-Clear Lake area, California: Thermal waters, mineralization, volcanism, and geothermal potential: ECONOMIC GEOLOGY, v. 88, p. 301–316.

Engebretson, D.C., Cox, A., and Gordon, R.G., 1982, Relative motions between oceanic and continental plates in the Pacific basin: Geological Society of America Special Paper 206, 59 p.

Field, C.W., and Fifarek, R.H., 1985, Light stable-isotope systematics in the epithermal environment: Reviews in Economic Geology, v. 2, p. 99–128.

Frisken, J.G., 1992, Interpretation of reconnaissance geochemical data from the Port Moller, Stepovak Bay, and Simeonof Island quadrangles, Alaska Peninsula, Alaska: U.S. Geological Survey Bulletin 1968, scale 1:250,000, 47 p.

Frost, T.P., 1990, Geology and geochemistry of mineralization in the Bethel quadrangle, southwestern Alaska: U.S. Geological Survey Bulletin 1950, p. C1–C9.

Globerman, B.R., and Coe, R.S, 1982, Preliminary paleomagnetic results from Late Cretaceous-early Tertiary volcanic rocks in the northern Bristol Bay coastal region, southwest Alaska [abs.]: EOS, v. 63, p. 915.

Godfrey, J.D., 1962, The deuterium content of hydrous minerals from the east-central Sierra Nevada and Yosemite National Park: Geochimica et Cosmochimica Acta, v. 26, p. 1215–1245.

Goldfarb, R.J., Gray, J.E., and Tripp, R.B., 1988, Geochemical anomalies in the eastern Katmai region of the Alaskan Peninsula: U.S. Geological Survey Circular 1016, p. 132–135.

Goldfarb, R.J., Gray, J.E., Pickthorn, W.J., Gent, C.A., and Cieutat, B.H., 1990, Stable isotope systematics of epithermal mercury-antimony mineralization, southwestern Alaska: U.S. Geological Survey Bulletin 1950, p. E1–E9.

Govett, G.J.S., 1983, Rock geochemistry in mineral exploration: Handbook of exploration geochemistry: New York, Elsevier, v. 3, 461 p.

Gray, J.E., Frost, T.P., Goldfarb, R.J., and Detra, D.E., 1990, Gold associated with cinnabar- and stibnite-bearing deposits and mineral occurrences in the Kuskokwim River region, southwestern Alaska: U.S. Geological Survey Bulletin 1950, p. D1–D6.

Gray, J.E., Goldfarb, R.J., Detra, D.E., and Slaughter, K.E., 1991, Geochemistry and exploration criteria for cinnabar-stibnite epithermal vein systems in the Kuskokwim River region, southwest Alaska: Journal of Geochemical Exploration, v. 41, p. 363–386.

Gray, J.E., Goldfarb, R.J., Snee, L.W., and Gent, C.A., 1992, Geochemical and temporal conditions for the formation of mercury-antimony deposits, southwestern Alaska [abs.]: Geological Society of America Abstracts with Programs, v. 24, p. 28.

Gray, J.E., Theodorakos, P.M., Bradley, L.A., and Bullock, J.H., Jr., 1993, Favorable areas for metallic mineral resources in and near the Horn Mountains, Sleetmute quadrangle, southwestern Alaska: U.S. Geological Survey Bulletin 2068, p. 79–90.

Green, C.B., Bundtzen, T.K., Peterson, R.J., Seward, A.F., Deagen, J.R., and Burton, J.E., 1989, Alaska's mineral industry, 1988: Alaska Division of Geological and Geophysical Surveys Special Report 43, 79 p.

Grinenko, V.A., 1962, Preparation of sulfur dioxide for isotope analysis: Zhurnal Neorganicheskoi Khimii, v. 7, p. 2478–2483.

Gustafson, D.L., 1991, Anatomy of a discovery: The McLaughlin gold mine, Napa, Yolo, and Lake Counties, California: ECONOMIC GEOLOGY MONOGRAPH 8, p. 350–359.

Hawley, C.C., Martinez, E.E., and Marinenko, J.W., 1969, Geochemical data on the south ore zone, White Mountain mine, and on the gold content of other mercury ores, southwestern Alaska: U.S. Geological Survey Circular 615, p. 16–20.

Hayba, D.O., Bethke, P.M., Heald, P., and Foley, N.K., 1985, Geologic, mineralogic, and geochemical characteristics of volcanic-hosted epithermal precious-metal deposits: Reviews in Economic Geology, v. 2, p. 129–167.

Herreid, G., 1960, Geology of the Red Devil quicksilver mine, Alaska [abs.]: Geological Society of America Abstracts with Programs, v. 71, p. 2086.

Hill, J.M., 1933, Lode deposits of the Fairbanks district, Alaska: U.S. Geological Survey Bulletin 849-B, p. 19–163.

Hillhouse, J.W., Grommé, C.S., and Csejtey, Béla, Jr., 1985, Tectonic implications of paleomagnetic poles from early Tertiary volcanic rocks, south-central Alaska: Journal of Geophysical Research, v. 90, p. 12523–12535.

Hoare, J.M., and Coonrad, W.L., 1959, Geology of the Bethel quadrangle, Alaska: U.S. Geological Survey Miscellaneous Geologic Investigations Map I-285, scale 1:250,000.

Jasper, M.W., 1955, Kolmakof cinnabar prospect: Property examination: Alaska Territorial Department of Mines Property Examination Report PE 82–4, 14 p.

Jones, D.L., Silberling, N.J., Coney, P.J., and Plafker, G., 1987, Lithotectonic terrane map of Alaska (west of the 141st meridian): U.S. Geological Survey Miscellaneous Field Studies Map MF-1874-A, scale 1:2,500,000.

Knappen, R.S., 1929, Geology and mineral resources of the Aniakchak district: U.S. Geological Survey Bulletin 797-F, p. 161–227.

Krupp, R., 1988, Physicochemical aspects of mercury metallogenesis: Chemical Geology, v. 69, p. 345–356.

Kulla, J.B., and Anderson, T.F., 1978, Experimental oxygen isotope fractionation between kaolinite and water: U.S. Geological Survey Open-File Report 78–701, p. 234–235.

Landis, G.P., and Hofstra, A.H., 1991, Fluid inclusion gases chemistry as a potential minerals exploration tool: Case studies from Creede, CO, Jerritt Canyon, NV, Coeur d'Alene district, ID and MT, southern Alaska mesothermal veins, and mid-continent MVT's: Journal of Geochemical Exploration, v. 42, p. 25–59.

Lehrman, N.J., 1986, The McLaughlin mine, Napa and Yolo counties, California: Nevada Bureau of Mines and Geology Report 41, p. 85–89.

Lindgren, W., 1933, Mineral deposits, 4th ed.: New York, McGraw-Hill, 930 p.

Longstaffe, F.J., 1987, Stable isotope studies of diagenetic processes: Mineralogical Association of Canada Short Course Handbook, v. 13, p. 187–257.

MacKevett, E.M., Jr., and Berg, H.C., 1963, Geology of the Red Devil quicksilver mine, Alaska: U.S. Geological Survey Bulletin 1142-G, p. G1–G16.

Malone, K., 1962, Mercury occurrences in Alaska: U.S. Bureau of Mines Information Circular 8131, 57 p.

Martin, G.C., 1905, Gold deposits of the Shumagin Islands: U.S. Geological Survey Bulletin 259, ser. A, p. 100–101.

McGimsey, R.G., Miller, M.L., and Arbogast, B.F., 1988, Analytical results and sample locality map of rock samples from the Iditarod quadrangle, Alaska: U.S. Geological Survey Open-File Report 88–421-A, scale 1:250,000, 110 p.

McKee, E.H., Noble, D.C., and Vidal, C., 1986, Timing of volcanic and hydrothermal activity, Huancavelica mercury district, Peru: ECONOMIC GEOLOGY, v. 81, p. 489–492.

Merrill, C.W., and Maloney, R.P., 1974, Kolmakof mercury deposits: U.S. Bureau of Mines Open-File Report 21–75, 19 p.

Mertie, J.B., Jr., 1918a, Lode mining in the Fairbanks district, Alaska: U.S. Geological Survey Bulletin 662, p. 403–424.

—— 1918b, Lode mining on Seward Peninsula, Alaska: U.S. Geological Survey Bulletin 662, p. 425–449.

—— 1936, Mineral deposits of the Ruby-Kuskokwim region, Alaska: U.S. Geological Survey Bulletin 864-C, p. 115–247.

Metz, P.A., 1977, Comparison of the mercury-antimony-tungsten mineralization of Alaska with stratabound cinnabar-stibnite-scheelite deposits of the Circum-Pacific and Mediterranean regions: Alaska Division of Geological and Geophysical Surveys Geologic Report 55, Short Notes on Alaskan Geology-1977, p. 39–41.

Metz, P.A., and Robinson, M.S., 1980, Investigation of mercury-antimony-tungsten metal provinces of Alaska: University of Alaska Mineral Industry Research Laboratory Open-File Report 80–8, p. 153–190.

Miller, M.L., and Bundtzen, T.K., 1994, Generalized geologic map of the Iditarod quadrangle, Alaska, showing potassium-argon, major-oxide, trace-element, fossil, paleocurrent, and archaeological sample localities: U.S. Geological Survey Miscellaneous Field Studies Map MF-2219-A, scale 1:250,000, 48 p.

Miller, M.L., Belkin, H.E., Blodgett, R.B., Bundtzen, T.K., Cady, J.W., Goldfarb, R.J., Gray, J.E., McGimsey, R.G., and Simpson, S.L., 1989, Pre-field study and mineral resource assessment of the Sleetmute quadrangle, southwestern Alaska: U.S. Geological Survey Open-File Report 89–363, 115 p.

Mining Journal, 1987, Shumagin results evaluation: v. 309, p. 328.

Moll, E.J., and Patton, W.W., Jr., 1982, Preliminary report on the Late Cretaceous and early Tertiary volcanic and related plutonic rocks in western Alaska: U.S. Geological Survey Circular 844, p. 73–76.

Moll-Stalcup, E.J., 1994, Latest Cretaceous and Cenozoic magmatism in mainland Alaska: Boulder, Colorado, Geological Society of America, Geology of North Amereica, v. G1, p. 589–619.

Nokleberg, W.J., Bundtzen, T.K., Berg, H.C., Brew, D.A., Grybeck, D., Robinson, M.S., Smith, T.E., and Yeend, W., 1987, Significant metalliferous lode deposits and placer districts of Alaska: U.S. Geological Survey Bulletin 1786, 104 p.

Ohmoto, H., and Rye, R.O., 1979, Isotopes of sulfur and carbon, *in* Barnes, H.L., ed., Geochemistry of hydrothermal ore deposits, 2nd ed.: New York, John Wiley, p. 509–567.

O'Neil, J.R., Clayton, R.N., and Mayeda, T., 1969, Oxygen isotope fractionation in divalent metal carbonates: Journal of Chemical Physics, v. 51, p. 5547–5558.

Peabody, C.E., 1993, The association of cinnabar and bitumen in mercury deposits of the California Coast Ranges: Society for Geology Applied to Mineral Deposits Special Publication 9, p. 178–209.

Peabody, C.E., and Einaudi, M.T., 1992, Origin of petroleum and mercury in the Culver-Baer cinnabar deposit, Mayacmas district, California: ECONOMIC GEOLOGY, v. 87, p. 1078–1103.

Pearcy, E.C., and Petersen, U., 1990, Mineralogy, geochemistry and alteration of the Cherry Hill, California hot-spring gold deposit: Journal of Geochemical Exploration, v. 36, p. 143–169.

Randolph, D.B., 1991, Unalaska project 1990: Final report, Battle Mountain Exploration Company, Alaska district: Anchorage, Alaska, The Aleut Corporation, unpublished report, 62 p.

Rea, D.K., and Duncan, R.A., 1986, North Pacific plate convergence: A quantitative record of the past 140 m.y.: Geology, v. 14, p. 373–376.

Robinson, M.S., and Decker, J., 1986, Preliminary age dates and analytical data for selected igneous rocks from the Sleetmute, Russian Mission, Taylor Mountains, and Bethel quadrangles, southwestern Alaska: Alaska Division of Geological and Geophysical Surveys Public-Data File 86–99, 9 p.

Roedder, E., 1963, Studies of fluid inclusions, 2. Freezing data and their interpretation: ECONOMIC GEOLOGY, v. 58, p. 167–211.

Roedder, E., 1979, Fluid inclusions as samples of ore fluids, *in* Barnes, H.L., ed., Geochemistry of hydrothermal ore deposits, 2nd ed.: New York, John Wiley, p. 684–737.

Romberger, S.B., 1988, Geochemistry of gold in hydrothermal deposits: U.S. Geological Survey Bulletin 1857, p. A9–A25.

Rose, A.W., Hawkes, H.E., and Webb, J.S., 1979, Geochemistry in mineral exploration, 2nd ed.: New York, Academic Press, 657 p.

Rytuba, J.J., 1986, Descriptive model of hot-spring Hg: U.S. Geological Survey Bulletin 1693, p. 178–179.

Rytuba, J.J., Hernandez, A.M., Rye, R.O., Dean, J.A., and Arribas, A., 1989, Genesis of Almaden type mercury deposits, Almaden, Spain [abs.]: International Geological Congress, 28th, Washington, D.C., July 9–19, 1989, Abstracts, v. 2, p. 2–741.

Sainsbury, C.L., and MacKevett, E.M., Jr., 1965, Quicksilver deposits of southwestern Alaska: U.S. Geological Survey Bulletin 1187, 89 p.

Saupé, F., and Arnold, M., 1992, Sulphur isotope geochemistry of the ores and country rocks at the Almaden mercury deposit, Ciudad Real, Spain: Geochimica et Cosmochimica Acta, v. 56, p. 3765–3780.

Savin, S.M., and Epstein, S., 1970, The oxygen and hydrogen isotope geochemistry of clay minerals: Geochimica et Cosmochimica Acta, v. 34, p. 25–42.

Seward, T.M., 1984, The transport and deposition of gold in hydrothermal systems: Geological Society of Zimbabwe Special Publication 1, p. 165–181.

Sheppard, S.M.F., 1986, Characterization and isotopic variations in natural waters: Reviews in Mineralogy, v. 16, p. 165–183.

Sherlock, R.L., and Jowett, E.C., 1992, The McLaughlin hot-spring gold-mercury deposit and its relationship to hydrothermal systems in the Coast Ranges of northern California, USA: International Symposium on Water-Rock Interaction, 7th, Park City, Utah, July 13–18, 1992, Proceedings, v. 2, p. 979–982.

Shew, N., and Wilson, F.H., 1981, Map and table showing radiometric ages of rocks in southwestern Alaska: U.S. Geological Survey Open-File Report 81–886, scale 1:1,000,000, 25 p.

Sillitoe, R.H., 1979, Some thoughts on gold-rich porphyry copper deposits: Mineralium Deposita, v. 14, p. 161–174.

—— 1991, Gold metallogeny of Chile: An introduction: ECONOMIC GEOLOGY, v. 86, p. 1187–1205.

Smith, P.S., and Maddren, A.G., 1915, Quicksilver deposits of the Kuskokwim region: U.S. Geological Survey Bulletin 622, p. 272–291.

Snee, L.W., Sutter, J.F., and Kelley, W.C., 1988, Thermochronology of economic mineral deposits: Dating the stages of mineralization at Panasqueira, Portugal, by high-precision $^{40}Ar/^{39}Ar$ age spectrum techniques on muscovite: ECONOMIC GEOLOGY, v. 83, p. 335–354.

Sorg, D.H., and Estlund, M.B., 1972, Geologic map of the mountain top mercury deposit southwestern Alaska: U.S. Geological Survey Miscellaneous Field Studies Map MF-449, scale 1:250,000.

Spurr, J.E., 1900, A reconnaissance in southwestern Alaska in 1898: U.S. Geological Survey Twentieth Annual Report, pt. 7, p. 31–264.

Spycher, N.F., and Reed, M.H., 1989, Evolution of a Broadlands-type epithermal ore fluid along alternative P-T paths: Implications for the transport and deposition of base, precious, and volatile metals: ECONOMIC GEOLOGY, v. 84, p. 328–359.

Szumigala, D.J., 1993, Gold mineralization related to Cretaceous-Tertiary magmatism in the Kuskokwim Mountains of west-central and southwestern Alaska: Unpublished Ph.D. dissertation, Los Angeles, California, University of California, 301 p.

Taylor, H.P., Jr., 1979, Oxygen and hydrogen isotope relationships in hydrothermal mineral deposits, *in* Barnes, H.L., ed., Geochemistry of hydrothermal ore deposits, 2nd ed.: New York, John Wiley, p. 236–277.

Taylor, H.P., Jr., and Epstein, S., 1962, Relation between O^{18}/O^{16} ratios in coexisting minerals of igneous and metamorphic rocks, 1. Principals and experimental results: Geological Society of America Bulletin, v. 73, p. 461–480.

Thrupp, G.A., and Coe, R.S., 1986, Early Tertiary paleomagnetic evidence and the displacement of southern Alaska: Geology, v. 14, p. 213–217.

Vallier, T.L., Scholl, D.W., Fisher, M.A., Bruns, T.R., Wilson, F.H., von Huene, R., and Stevenson, A.J., 1994, Geologic framework of the Aleutian arc, Alaska: Boulder, Colorado, Geological Society of America, Geology of North America, v. G1, p. 367–388.

Varekamp, J.C., and Buseck, P.R., 1984, The speciation of mercury in hydrothermal systems, with applications to ore deposition: Geochimica et Cosmochimica Acta, v. 48, p. 177–185.

Wallace, W.K., and Engebretson, D.C., 1984, Relationship between plate motions and Late Cretaceous to Paleogene magmatism in southwestern Alaska: Tectonics, v. 3, p. 295–315.

Wallace, W.K., Hanks, C.L., and Rogers, J.F., 1989, The southern Kahiltna terrane: Implications for the tectonic evolution of southwestern Alaska: Geological Society of America Bulletin, v. 101, p. 1389–1407.

Webber, B.S., Bjorklund, S.C., Rutledge, F.A., Thomas, B.I., and Wright, W.S., 1947, Mercury deposits of southwestern Alaska: U.S. Bureau of Mines Report of Investigations 4065, 57 p.

Wells, J.T., and Ghiorso, M.S., 1988, Rock alteration, mercury transport, and metal deposition at Sulphur Bank, California: ECONOMIC GEOLOGY, v. 83, p. 606–618.

White, D.E., 1957, Magmatic, connate, and metamorphic waters: Boulder, Colorado, Geological Society of America Bulletin, v. 68, p. 1659–1682.

—— 1967, Mercury and base-metal deposits with associated thermal and mineral waters, *in* Barnes, H.L., ed., Geochemistry of hydrothermal ore deposits: New York, Holt, Rinehart, and Winston, p. 575–631.

White, D.E., and Roberson, C.E., 1962, Sulphur Bank, California, a major hot spring quicksilver deposit, *in* Engel, A.E.J., James, H.L., and Leonard, B.F. eds., Petrological studies: A volume in honor of A.F. Buddington: Boulder, Colorado, Geological Society of America, p. 397–428.

White, D.E., Barnes, I., and O'Neil, J.R., 1973, Thermal and mineral waters of non-meteoric origin, California Coast Ranges: Geological Society of America Bulletin, v. 84, p. 547–560.

White, W.H., and Queen, L.D., 1989, Preliminary geologic and rock-chip geochemical data from drill core and trenches at the Shumagin gold deposit, Unga Island, Alaska: U.S. Geological Survey Open-File Report 89-361, 11 p.

Wilson, F.H., 1980, Late Mesozoic and Cenozoic tectonics and the age of porphyry copper prospects, Chignik and Sutwik Island quadrangles, Alaska: U.S. Geological Survey Open-File Report 80–543, 94 p.

—— 1981, Map and table showing radiometric ages of rocks in the Aleutian Islands and Alaska Peninsula: U.S. Geological Survey Open-File Report 81–471, 23 p., 1 sheet, scale 1:1,000,000.

—— 1985, The Meshik arc: An Eocene to earliest Miocene magmatic arc on the Alaska Peninsula: Alaska Division of Geological and Geophysical Surveys Professional Report 88, 14 p.

Wilson, F.H., and Cox, D.P., 1983, Geochronology, geochemistry, and tectonic environment of porphyry mineralization in the central Alaska Peninsula: U.S. Geological Survey Open-File Report 83–783, 24 p.

Wilson, F.H., and Shew, N.B., 1992, Map and tables showing geochronology and whole-rock geochemistry of selected samples, Ugashik and part of Karluk quadrangles, Alaska: U.S. Geological Survey Miscellaneous Field Studies Map MF-1539-E, scale 1:250,000.

Wilson, F.H., Case, J.E., and Detterman, R.L., 1985, Preliminary description of a Miocene zone of structural complexity in the Port Moller and Stepovak Bay quadrangles, Alaska: U.S. Geological Survey Circular 945, p. 55–56.

Wilson, F.H., White, W.H., and DuBois, G.D., 1988, Brief descriptions of mines, prospects, and mineral occurrences in the Port Moller and Stepovak Bay quadrangles, Alaska Peninsula: U.S. Geological Survey Open-File Report 88–666, 128 p.

Wilson, F.H., Shew, N.B., DuBois, G.D., and Bie, S.W., 1994, Sample locality map and analytical data for potassium-argon ages in the Port Moller, Stepovak Bay, and Simeonof Island quadrangles, Alaska Peninsula: U.S. Geological Survey Miscellaneous Field Studies Map MF-2155-F, 18 p.

Wilson, F.H., White, W.H., Detterman, R.L., and Case, J.E., 1996, Maps showing the resource assessment of the Port Moller, Stepovak Bay, and Simeonof Island quadrangles, Alaska Peninsula: U.S. Geological Survey Miscellaneous Field Studies Map MF 2155-F.

Yanaglsawa, F., and Sakal, H., 1983, Thermal decomposition of barium sulfate-vanadium pentoxide-silica glass mixtures for preparation of sulfur dioxide in sulfur isotope ratio measurements: Analytical Chemistry, v. 55, p. 985–987.

Young, L.E., St. George, P., and Bouley, B., 1997, Porphyry copper deposits in relation to the magmatic history and palinspastic restoration of Alaska: ECONOMIC GEOLOGY MONOGRAPH 9, p. 306–333.